Kingsley Gideon Kumashie

Flow-cytometric Analysis of Autophagy in Activated Primary Human CD4+ T Cells

Master's Thesis in Molecular Medicine

Trondheim, 2015

Principal supervisor: Markus Haug, PhD

Co-supervisor: Trude Helen Flo, PhD

Norwegian University of Science and Technology

Faculty of Medicine

Department of Cancer Research and Molecular Medicine

NTNU – Trondheim
Norwegian University of
Science and Technology

Abstract

The hallmark of an immune response to *Mycobacterium tuberculosis* is granuloma formation. CD4+Th1 cells are of central importance in anti-mycobacterial immunity by way of producing effector IFN-γ and TNF-α cytokines that help to contain infection in the granulomas by activating macrophages. The environment of the granuloma is hypoxic and we have little knowledge on CD4+ T cell processes and function in this environment. Autophagy is a *de novo* intracellular protein and organelle degradation pathway induced in eukaryotic cells by stress-factors such as starvation or hypoxia. It has been described that autophagy is induced in T cells upon activation and autophagic processes might contribute to nutrient supply and the regulation of cytokine production in T cells. The aim of this study was to investigate autophagic processes in CD4+ T cells after activation and the regulation of IFN-γ production under normoxia, and hypoxia as found in the granuloma of TB patients.

The main assays, immunoblotting and confocal microscopy that are currently used to study autophagy, have the limitation of not easily allowing analysis of autophagy on different T cell subsets in a heterogeneous cell sample. In this study, autophagy was quantified in different subsets of CD4+ T cells by a flow-cytometric method using a novel fluorescent probe, the CytoID autophagy detection kit. The findings of the flow-cytometric method were validated by LC3 immunoblotting and then used to study different aspects of T cell activation on autophagy in primary human CD4+ T cells. In this regard, we have shown that the flow-cytometric method of autophagy analysis can be combined with fluorescent surface marker staining but not intracellular staining for effector cytokines. We have also demonstrated that TCR stimulation without co-stimulation induces autophagy in primary human CD4+ T cell. Further, we found increased autophagy in CD4+ T cell subsets expressing the activation marker CD25+ 48 and 72 h post activation and CD4+CD25+T cells were found to be the main producers of effector Th1 cytokines, providing indirect evidence that autophagy might be increased in cytokine-producing CD4+ effector T cells. Finally we have successfully established a novel way of quantifying autophagy in effector cytokine specific T cells using a fluorescent cytokine catch reagent independent of intracellular cytokine staining. Using this method we have shown that autophagy is strongly induced in cytokine (IFN-γ) producing CD4+ T cells. In addition, we have shown that hypoxia did not induce autophagy in unstimulated primary human CD4+ T cells. In contrast, autophagy,

surface activation marker and effector cytokine production were strongly upregulated in activated T cells under hypoxic conditions. All experiments in this study were performed with polyclonally activated CD4+ T cells. Therefore, we have developed an assay to expand mycobacteria-specific CD4+ T cell from healthy human donors in order to allow for future analysis of autophagy in antigen-specific CD4+ T cells.

The assays developed in this study may provide valuable tools in elucidating autophagy and effector Th1 cytokine regulation in antigen-specific T cells under different conditions such as hypoxia as seen *in vivo* in the granuloma of TB patients.

Acknowledgement

I would like to appreciate my supervisor Markus Haug, PhD for teaching me the basics of laboratory bench work, guidance and encouragement. Not forgetting Trude Flo, PhD for granting me the opportunity to work in her research group. I would like to thank them graciously.

I doff out my hat to Hany Ibrahim and Nisha Kannan for the numerous encouragement and believe in my abilities. More also, to Hany, I am grateful for teaching me western blot and ordering buffy coats for me as well as all the countless helps you offered.

A special thank you to Claire for isolating PBMCs for me sometimes and all the lab members Jane, Alex, Signe, Marte and Anne who have been part of this success story.

Finally, I would like to appreciate my colleague students Ida, Oda, Yohannes, Maja and Sindre for all the exciting and challenging moments we shared together whiles in the lab. It could not get any better without you.

Table of contents

List of Figures

Abbreviations

DCs: Dendritic cells

MHC: Major histocompatibility molecules

kDa: Kilo Daltons

Atg: Autophagy related genes

ULK: unc-51-like kinase

AMPK: Adenosine monophosphate protein kinase

mTOR: Mammalian target of rapamycin

ATP: Adenosine triphosphate

PI3K: Class III phosphatidylinositol 3-kinase

PIK3CS/VPS34: phosphatidylinositol 3-kinase, catalytic subunit 3

PIK3R4/p150: phosphatidylinositide 3-kinase, regulatory subunit 4

BECN1: Beclin 1

PtdIns3P: Phosphatidylinositol 3-phosphate

LC3: Microtubules associated light chain 3

PE: Phosphatidylethanolamine

IL-2: Interleukin 2

IFN-γ: Interferon gamma

TCR: T cell receptor

NFAT: Nuclear factor of activated T cells

AP-1: Activator protein-1

NF-kB: Nuclear factor-kB

PLCγ: Phospholipase C-γ

PIP2: Phosphatidylinositol-4,5-bisphosphate

IP3: Inositol-1,4,5-triphosphate

DAG: Diacylglycerol

PKC: Protein kinase C

ER: Endoplasmic reticulum

IKK: IkB kinase

Mtb: *Mycobacterium tuberculosis*

TB: Tuberculosis

TNFα: Tumor necrosis factor alpha

HIF-1α: Hypoxia inducible factor 1α

HIV: Human immunodeficiency virus

CQ: chloroquine

PBMCs: Peripheral blood mononuclear cells

MDMs: Monocyte-derived macrophages

MOI: Multiplicity of infection

CFU: Colony forming unit

HBSS: Hanks balanced salt solution

M-CSF: Macrophage colony-stimulating factor

EDTA: Ethylenediaminetetraacetic acid

1 Introduction

1.1 Autophagy

1.1.1 Mechanisms of autophagy

Autophagy is a highly conserved *de novo* intracellular homeostatic mechanism in eukaryotic cells which plays valuable roles in the degradation of waste components (e.g., long lived proteins or damaged organelles) in acidic lysosomal compartment. This is needed to provide nutrients and energy under conditions of stress (1, 2). This intracellular homeostatic process is a novel emerging aspect of the immune system and has been implicated in numerous function of the innate and adaptive immunity (3). Furthermore, it plays an important role in bridging the adaptive and the innate immune system by facilitating antigenic-peptide presentation unto major histocompatibility molecules (MHC) for enhanced T cell responses (4).

Three autophagy pathways have been described in mammalian cells. These consist of micro-autophagy, chaperone-mediated autophagy and macro-autophagy. Chaperone-mediated autophagy is involved in selective degradation of soluble cytosolic proteins. The cytosolic proteins to be degraded are selectively targeted by heat shock cognate protein of 70kDa, which facilitate the protein delivery across the lysosomal membrane (5). In micro-autophagy, cytosolic contents are sequestered into vesicles directly by lysosomal membrane invagination. These vesicles pinch off into the lumen of the lysosome and are then degraded. In contrast, macro-autophagy involves the formation of double membrane structure (autophagosome) around the targeted cytosolic cargos. The autophagosomes then fuses with lysosome to deliver their content for degradation (6). In all the above outlined pathways, macro-autophagy (herein referred to as autophagy) is the most described pathway which is suggested to play a well-defined role in immunity (Puleston & Simon, 2014).

1.1.2 Autophagy pathway

Four distinct processes are involved in autophagy: nucleation, elongation, fusion and degradation. Nucleation involves the formation of isolated double-membrane structure (called the phagophore). The phagophore is extended in the elongation phase which engulfs the cytosolic contents. The

phagophore then encloses its cargo forming the autophagosome (9). The autophagosome then fuses with the lysosome leading to the degradation of the autophagosome content by proteases and lipases within the lysosome. The degraded components are then released into the cytosol to provide for the metabolic function of the cell. Autophagy processes are mediated/controlled by a set of autophagy related (Atg) genes (8).

In mammalian cells, the onset of autophagy is initiated by the unc-51-like kinase (ULK) complex. This complex consists of core proteins ULK1 (or ULK2; hereafter referred to as ULK1), RB1CC1/FIP200 (RB1-inducible coiled-coil 1; the mammalian orthologous of Atg17), Atg13 and Atg101 (binds to Atg13 and has no known yeast ortholog), and is involved in the induction of autophagosome formation (9) (**Figure. 1.1**). The mammalian target of rapamycin (mTOR) complex 1 and adenosine monophosphate (AMP)-activated protein kinase (AMPK) are the key regulators of the ULK1 kinase complex (**Figure. 1.1**). Under energy deprivation AMPK is activated in cells, which acts in switching on autophagy to catabolize cellular components leading to adenosine triphosphate (ATP) generation. Nutrient insufficiency also turns off mTOR which results in upregulation of autophagy (**Figure 1.1**). This provides a mechanism to restore amino acid levels through the breakdown of proteins (10, 11).

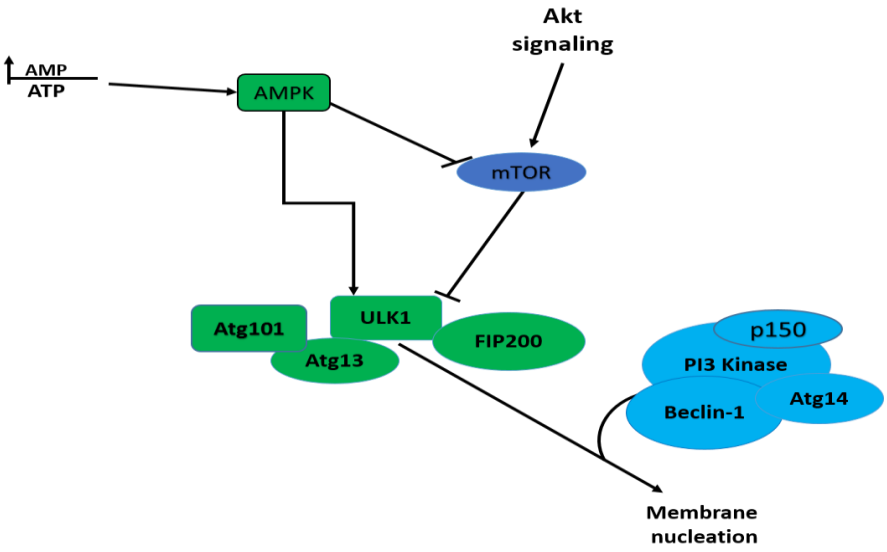

Figure 1.1: Schematic representation of the upstream signaling pathways prior to phagophore formation during autophagy
The mammalian target of rapamycin (mTOR) is under the control of Akt signaling and AMPK. Under energy deprivation, AMPK inhibits mTOR whiles stimulating ULK1 leading to phagophore formation via membrane nucleation. Signaling through Akt pathways activates mTOR. Activated

mTOR then inhibits ULK1 which results in down-regulation of phagophore formation. PI3K and ULK1 complexes coordinate to facilitate the formation of isolation membrane[*].

During phagophore nucleation, proteins and lipids are recruited for the processes that lead to autophagosome biogenesis. Class III phosphatidylinositol 3-kinase (PI3K) complex plays an essential role in the autophagy nucleation process. The complex consists of the core proteins PIK3CS/VPS34 (phosphatidylinositol 3-kinase, catalytic subunit 3), PIK3R4/p150 (phosphatidylinositide 3-kinase, regulatory subunit 4; the yeast orthologous is Vps15), BECN1 (Beclin 1; the yeast autologous is Vsp30/Atg6) and Atg14 (10). The class III PI3K complex is recruited to the autophagosome formation site during nucleation which then recruits phosphatidylinositol 3-phosphate (PI3P)-binding protein. This leads to the formation of isolation membrane at the endoplasmic reticulum (ER) site. PI3P produced by Vps34 recruits PI3P-binding effectors, which further enhances the formation of the isolation membrane (2, 8). A key function of PI3K complex is to generate PI3P that serve as a tag on the isolation membrane to recruit other factors involved in autophagosome formation. PI3K complex regulation occurs to a large extent through host factor (eg. Atg14) interaction with BECN1 (10).

Following nucleation, the phagophore is elongated into a closed autophagosome through the action of microtubules associated light chain 3 (LC3). LC3 is a prototypic marker of autophagosome and a product of two ubiquitin-like conjugation systems (2). The first of these is the covalent Atg12-Atg5 conjugation system which is made up of Atg12 (ubiquitin-like protein), Atg7 (E1-like enzyme), Atg10 (E2-like enzyme), Atg5 and Atg16L (**Figure 1.2**). Atg16L1 anchors Atg12-Atg5 complex into the growing autophagosome and acts as an E3-like enzyme, which promotes the conjugation of LC3 to phosphatidylethanolamine (PE) (10). The Atg12-Atg5-Atg16L1 complex facilitates the localization of the second conjugation system (LC3 conjugation system) into the isolation membrane. Prior to the localization, LC3 is activated by Atg7 and then coupled to PE by Atg3 to form LC3-PE (also referred to as LC3II). The LC3 conjugation system is made up of LC3 (ubiquitin-like protein), Atg7 (E1-like enzyme) and Atg3 (E2-like enzyme) (12). Two subfamilies of the LC3 protein orthologs have been described in mammals: LC3 and Gamma-aminobutyric acid receptor-associated proteins (GABARAPs). These function during early and late

[*] Figure by the author

autophagosome elongation respectively (13). LC3-II then insert into the isolation membrane and assist its elongation into a closed autophagosome. Finally, the autophagosome fuses with late endosome or lysosome to form a digestive compartment called the autophagolysosome (14) (**Figure 1.2**). Furthermore, Atg4, a cysteine protease is involved in delipidation of LC3II on the outer membrane of autophagolysosomes. LC3II delipidation involves cleaving LC3 from the cytosolic surface of autophagosome (from its binding lipid) making it available for subsequent autophagosome formation (2, 8).

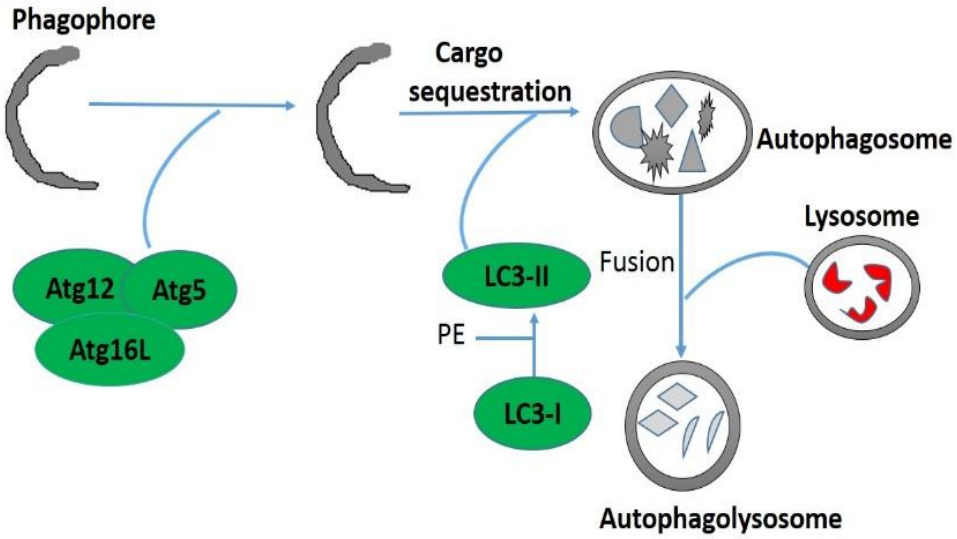

Figure 1.2: Schematic diagram of the autophagy pathway
The prototypic marker of autophagy LC3 is under the control of two ubiquitin-like conjugation enzymes Atg12-Atg5-Atg16L and LC3 conjugation system (Atg7-Atg3-LC3) (not shown). Atg16L which is part of the Atg12-Atg5-Atg16L conjugation system function as a docking site for Atg12-Atg5 on the phagophore, which facilitates the localization of LC3 conjugation system into the phagophore. Atg7-Atg3-LC3 make up the second conjugation system. In this conjugation system, LC3 is activated by Atg7 and coupled to PE by Atg3. The LC3-PE (LC3II) then incorporation into the phagophore leading to autophagosome formation. The formed autophagosome engulfs it sequestered cargo and then fuses with lysosome (autophagolysosome) resulting in cargo degradation by lysosomal hydrolases[†].

[†] Figure by the author

1.1.3 Autophagy in T cells

T cells originate from hematopoietic stem cell and mature in the thymus (15). Maturation involves a transition from double negative to double positive thymocyte, which is associated with differentiation stages and receptor gene rearrangement. Double positive thymocytes which interacts with intermediate avidity to self-peptide complexed to MHC molecules are positively selected (15, 16). Positively selected thymocytes are then committed to single positive CD4 or CD8 thymocytes. Single positive thymocytes (CD4+ or CD8+ T cells) then migrate into the medulla where they are negatively selected. Negative selection eliminates thymocytes which have a high affinity T cell receptor (TCR) to self-antigens, thereby reducing the probability of autoimmune pathologies (17, 18). All the processes involved in T cell development have been shown to be regulated by autophagy (reviewed in refs 8). The existence of autophagy in T cells points to a probable regulatory role for autophagy in the intracellular program of T cells. Autophagy vacuole accumulation were observed in aging T cells (19, 20) and an *in vitro* study where CD8+T cells were cultured for a long period of time showed progressive intolerance to activation (21). This intolerance to activation led to increased cell death, and also cell aging resulted in increased percentage of cells with autophagosome and lipofuscin accumulation.

T cell receptor stimulation with antigenic-peptides presented by MHC molecules on antigen-presenting cells (APCs) mediates the activation signals of T cells. TCR stimulation has been demonstrated to be a strong inducer of autophagy (22). In resting T cells, mitochondria are most often contained in the autophagosomes, but upon T cell activation, the autophagic cargo switches to cytosolic materials exclusively (22). Autophagy as a result of TCR stimulation requires key autophagy machinery. This is because, deleting Atg5, Atg7 and Atg3 can abolish autophagosome induction in T cells (19, 22). Furthermore, an early study demonstrated different level of autophagy in T helper (Th) 2 and Th1 effector CD4+ cells (20). In this study, it was reported that Th2 cell exhibited more autophagy than Th1 cells. The class III PI3K, Vps34 is required for T cell development and survival, however, the role of Vps34 for T cell survival is independent of autophagy (23). Furthermore, T cell receptor induced autophagy was found to be defective in aged CD4+ T cells (24). However, the precise mechanisms behind defective autophagy during T cell aging is not clear. But some evidence points to a probable p65 involvement, due to impaired

nuclear translocation of p65 upon TCR signaling. p65 has also been shown to be essential for autophagy induction via upregulating the transcription of BECN-1 in multiple cell lines (25).

1.1.4 Autophagy in antigen-presentation

T cells recognize foreign antigens presented on MHC molecules. Antigen-presentation is the pathway leading to effective delivery of antigenic-peptides to MHC molecules. All nucleated cells express MHCI molecules on their surfaces whereas MHCII molecules are expressed on professional APCs (macrophages, monocytes and dendritic cells) (26). MHCI molecules present peptides derived from intracellular compartments such as viral protein, cytoplasmic and nuclear self-antigens which are recognized by CD8+ T cells (27). During MHCI presentation, antigens are processed into peptides by proteasomes. These peptides are then transported into the ER through the transporter-associated with antigen presentation and then loaded onto MHCI molecule. The peptide-MHCI complex is then routed to the cell surface via the Golgi apparatus. CD4+ T cells on the other hand recognize antigens presented on MHCII molecules which are only expressed on professional APCs and epithelial cells (28). Like MHCI, MHCII synthesis occurs in the ER and it is associated with an invariant chain, which facilitates proper folding, trafficking and protection of the antigen binding groove. After assembly, MHCII molecules are trafficked to endolysosomal compartments where antigenic peptides are supplied for loading onto the antigen binding grooves. After peptide loading, the MHCII peptide complexes are delivered to the cell surface (26).

Autophagy aids intracellular and extracellular antigen processing for MHCI and II presentation and is implicated in cross-presentation processes. Cross-presentation processes are exclusively described in macrophages and dendritic cells and enable presentation of endogenously sourced antigen on MHC II and exogenously-sourced antigens on MHCI molecules (29). Autophagy has also been shown to contribute to MHCI presentation of herpes simplex virus-1 antigens (30). Pathogens such as mycobacteria can be targeted to autophagosomes, and converge with endosomes. This delivers antigens for loading into MHCII compartment. Autophagy can deliver endogenously generated antigens from for examples viruses for cross-presentation via the MHCII pathway (4) enhancing presentation to CD4+ T cells (31, 32). *In vivo* studies have shown that autophagy is important for MHCII presentation of self-proteins during central tolerance induction (33).

1.1.5 Activation of T cell and autophagy

Full activation of T cells requires three signals: TCR stimulation, co-stimulation via CD28 and IL-2 signaling (**Figure 1.3**). When these three signals are received, T cells switch their metabolic activity from catabolic oxidative phosphorylation to anabolic glycolysis and glutaminolysis. T cells which do not receive CD28 signaling upon TCR stimulation cannot upregulate glycolysis and glutaminolysis and becomes anergic (34, 35). Anergic T cell fail to proliferate when TCR is engaged without co-stimulation and are unable to produce cytokines such as interleukin 2 (IL-2) and interferon-gamma (IFN-γ) upon re-challenge with both anti-CD3 and anti-CD28. T cells which are fully activated induces signaling through Akt/mTOR, which is essential for T cell activation, and inhibition of mTOR renders activated T cells anergic (36). Signaling through Akt/mTOR may have consequences on autophagy since mTOR inhibits autophagy (**Figure 1.1**). However, increase in calcium level shortly after TCR triggering activates AMPK, which inhibits mTOR and induce catabolic metabolism (37). Autophagy is regulated by both mTOR and AMPK through the phosphorylation of ULK1 (11).

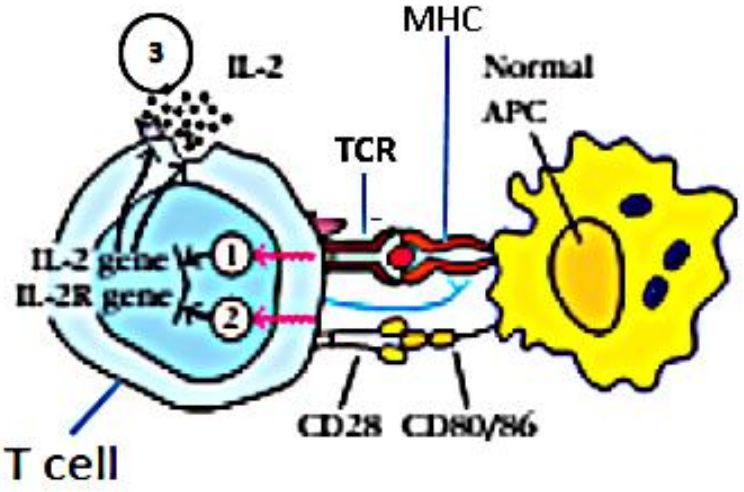

Figure 1.3: The three signals required for full T cell activation
Signal one is through T cell receptor stimulation via MHCs, signal two is received through CD28 by interacting with CD80/86 on APCs. Signals one and two cooperate to facilitate the transcription and stabilization of IL-2 and IL-2 receptor (IL-2R). Secreted IL-2 binds to IL-2R and generates signals (signal three) which enhances T cell entry into the cell cycle to initiate proliferation. Adapted and modified from (38).

Autophagy is involved in the metabolic activity of activated T cells. Upon TCR stimulation, T cells go through a metabolic switch to produce enormous amount of ATP to sustain the energy levels for protein synthesis, cytokine production and secretion, and cell division (39). The amount of ATP produced in activated CD4+ T cells has been shown to decrease when autophagy was blocked. Further, autophagy deficient CD4+ T cells were shown to have defective production of IL-2 and IFN-γ, and reduced proliferation after TCR stimulation. The defect in ATP and activation induced IFN-γ and IL-2 production was partially restored when methyl pyruvate, an intermediate of glucose metabolism was supplied to the autophagy deficient CD4+ T cells (22).

1.1.6 TCR downstream signaling

TCR stimulation leads to the activation of phospholipase C-γ (PLCγ), via the action of a receptor tyrosine kinase. The three important transcription factors induced upon full T cell activation are nuclear factor of activated T cells (NFAT), activator protein-1 (AP-1) and nuclear factor-kB (NF-kB). These regulate the transcription of important effector genes in T cells (40). Activated PLCγ after TCR triggering hydrolyze phosphatidylinositol-4,5-bisphosphate (PIP2) to produce inositol-1,4,5-triphosphate (IP3) and diacylglycerol (DAG). IP3 binds to its receptor on the ER leading to the release of calcium from intracellular calcium store. The released calcium triggers the opening of plasma membrane calcium channels, resulting in the influx of extracellular calcium (41). The elevated calcium level facilitates the recruitment of protein kinase C (PKC) to the plasma membrane, where it is activated by DAG. The activated PKC then stimulate IkB kinase (IKK), resulting in IKK activation. Activated IKK then phosphorylates IkB, leading to the ubiquitination and proteolysis of IkB thereby activating NF-kB. NF-kB then dimerize and translocate into the nucleus to transcribe genes involved in inflammatory responses (42).

NFAT is a family of highly phosphorylated proteins residing in the cytoplasm of resting T cells. When T cells are activated, these proteins are dephosphorylated by the calcium calmodulin-dependent phosphatase calcineurin, after which they translocate into the nucleus and become active transcription factors (43). NFAT cooperates with AP-1 in the nucleus to induce large numbers of cytokine genes. AP-1 is also a transcription factor which is at low level in unstimulated

cells (44). Upon TCR stimulation, AP-1 is induced and is activated by IKK via PKC signaling (45). In the absence of AP-1, NFAT induces the transcription of genes encoding negative regulators of T cell responses and induces anergy (46). Co-stimulatory molecules are not coupled to calcium mobilization and contribute weakly to NFAT activation. Thus, NFAT activation occurs through calcium signaling upon TCR stimulation via signal one alone (40, 47). Combination of TCR and CD28 stimulation activates cJun kinase (JNK), p38 mitogen activated protein (MAP) kinase, and IkB kinase (IKK) pathways and increases the level of nuclear NF-kB and AP-1 protein more strongly than TCR stimulation alone (40).

1.1.7 Effector CD4+ T cell subsets

After activation (**1.1.5**), CD4+T cells differentiate into different effector subset depending on the cytokines in the microenvironment, as well as on the antigen concentration, type of APCs and costimulatory molecules (48). Effector CD4+ T cells include Th1, Th2, T regulatory (T reg), T helper 17 (Th17) and T follicular helper (Tfh) cells. These effector cells play central roles in immune regulation and protection. Th1 cells mediate immune responses against intracellular pathogens and Th1 signature cytokines are IFN-γ, TNF, lymphotoxins-α and IL-2 (49). In contrast, Th2 cells mediate host immune responses against extracellular parasites and Th2 cells produce cytokines such as IL-4, IL-5, IL-10 and IL-13 (49). Furthermore, pro-inflammatory Th17 cells are involved in immune responses against extracellular bacteria and fungi. Th17 produce IL-17, IL-21 and IL-22 (48, 49). T reg cells play valuable roles in regulating immune responses and the maintenance of self-tolerance. T reg cell cytokines include transforming growth factor β, IL-10 and IL-35. Finally, Tfh cells provide T cell help to B cells and are important for germinal center formation, affinity maturation and the development of high affinity antibodies by B cells. Features which distinguish Tfh cells from other Th cells include the high expression of inducible T cell costimulator, CD40L and the cytokine IL-21 (50, 51).

1.2 *Mycobacterium tuberculosis* infection

Mycobacterium tuberculosis (Mtb) is the causative agent of tuberculosis (TB) and it belongs to the genus *Mycobacterium* (52). TB is transmitted through the inhalation of aerosol Mtb droplets that are suspended in the air for prolonged period of time (53). It has been reported that 3-10 % of immunocompetent individuals infected develop TB disease during their life time, while well over 90 % of infected individuals contain infection in a subclinical stage referred to as latent TB infection (54). Mtb is the most successful intracellular pathogen in view of its global distribution and prevalence. Mtb is ranked second as a single infectious agent causing death after infections with Human Immunodeficiency Virus (HIV) (55). Indeed, the World Health Organization (WHO) has estimated 9 million new TB cases in 2013 with 1.5 million deaths globally (including 360,000 deaths among HIV infected individuals). It has been proposed that one-third of the worlds' population is latently infected with Mtb (56).

1.2.1 Innate Immune responses to *Mycobacterium tuberculosis*

Following Mtb infection in the airways or lung parenchyma, the bacteria are believed to be engulfed by resident alveolar macrophages (52). Pattern recognition receptors such as Toll-like receptors, scavenger receptors and mannose receptors on alveolar macrophages recognizes pathogen-associated molecular patterns on mycobacterial surfaces leading to the bacilli been engulfed (57). In these cells, Mtb resides and may multiply within host derived phagosomes. The alveolar macrophages then secrete chemokines which recruits monocyte-derived macrophages and dendritic cells (DCs) (58) to the site of infection. In the course of time, these cells form a compact, organized aggregate structure of mature macrophages surrounded by fibroblast and interspersed with neutrophils, natural killer cells, B cells, CD4+ and CD8+ T cells (**Figure 1.4**). This structure is referred to as granuloma and has been suggested to be used by the immune system to sequester, wall off and eradicate Mtb. However, recent report has suggested otherwise. Indeed, granulomas may be structures exploited by Mtb at the initial stage of infection to subvert immune responses, replicate and spread to other location (55, 59). Mtb disease and hypoxia may potentiate each other. The environment of granuloma associated with Mtb infection are hypoxic. This has led to the

suggestion that the relative hypoxia of granulomas is a contributing factor to the latent infection phenotype and the associated relative resistance of Mtb to host effector mechanisms. The effect of hypoxia on host immune cell signaling is predominantly through the stabilization of hypoxia inducible factor 1 alpha (HIF-1α) transcription factor (60, 61).

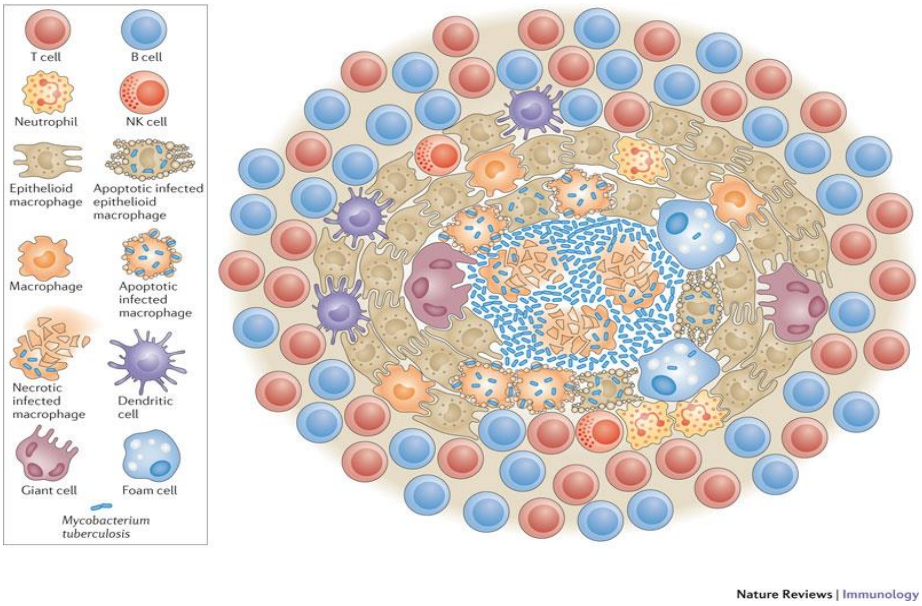

Figure 1.4: A schematic representation of TB granuloma
The granuloma consists of a necrotic core. The necrotic core is made up of macrophages which have differentiated into foam cells, characterized by lipid accumulation. The bacilli are commonly present in the central necrotic core area in which dead and dying macrophages can be seen. Other cell types such as neutrophils, dendritic cells, B and T cells, NK and fibroblast cells populate the granuloma (Figure adapted from (59).

The processes leading to the bacteria been taken-up (engulfed) by phagocytic cells is referred to as phagocytosis**.** Phagocytosis is a membrane invagination process resulting in phagosome formation (57, 62). The phagosomes formed undergo a maturation process where microbes contained in the phagosome are under the assault of increasing acidity, reactive oxygen and nitrogen species, hydrolytic enzymes and cationic antimicrobial peptides. The maturing phagosomes' acidic pH activates proteases and lipases that degrades proteins and lipids respectively, leading to the suppression of the metabolic activity of the bacilli (57, 63, 64). The

final step in microbial destruction and clearance is the fusion of phagosome with lysosome (52). Even though the innate immune system have developed all these arsenals of protective mechanisms to fight bacterial infections, Mtb has devised ways to escape these mechanisms and persist within phagocytic cells. These escape mechanisms includes but not limited to evasion of apoptosis and innate immune signaling, inhibition of autophagy, phagosomal maturation arrested at pH 6.4 and translocation from phagosomes into the cytosol of macrophages (52, 65, 66). Evidence accumulating suggest that autophagy in phagocytic cells may be an important effector mechanism that control the growth of mycobacteria (66), through enhanced phagosome maturation, which may trigger mycobacteria killing (67).

1.2.2 Initiation of an adaptive immune response to *Mycobacterium tuberculosis*

The adaptive immune response elicited against Mtb is T cell dependent and it is initiated by DCs. Upon antigen recognition, DCs process and present peptides on MHC molecules, upregulates chemokine receptors and migrate into local lymph node (68). The peptide-complex MHC molecules are recognized by T cells. In the peripheral lymphoid organs, naive T lymphocytes circulate looking for antigen which are processed and presented on MHC molecules by professional APCs. After peptide-complex MHC recognition, T cells undergoes rapid clonal expansion. Clonal expansion generates copious amount of specific T lymphocytes and results in memory formation. Memory lymphocytes are known to confer immediate protection and mount recall responses to antigens in secondary lymphoid organs (69). T cell protective memory is mediated by effector memory T cells (T_{EM}). T_{EM} migrate to inflamed peripheral tissues and immediately display effector functions. In contrast, reactive memory is mediated by central memory T cells, which home to T cell zones of the secondary lymphoid organ, have little or no effector function but upon response to antigenic stimulation they readily proliferate and differentiate into effector cells (68).

The initiation of adaptive immune response to Mtb might not be able to clear infection or to provide sterile immunity. Nevertheless, it is important to prevent reactivation at later stages of infection. A characteristic feature of developing an adaptive immunity to TB is its long interval compared to responses to immunization or other bacterial infections (70, 71). The mechanisms that account for

delayed adaptive immune response to TB are not well understood (70). Suggestions put forward to explain the delayed adaptive immune response to Mtb infection are as follow: (1) slow bacterial growth which leads to delayed antigen accumulation in the lungs, (2) delayed trafficking of antigen to peripheral lymph organs, (3) interference with antigen presentation pathway, and (4) delayed recruitment and migration of lymphocytes to infected sites (71). Recent *in vitro* studies showed that DCs exposed to Mtb caused a decrease in the expression of integrin subunits. Decreased integrin expression in DCs were associated with impaired DC adhesion to endothelial cells and migration toward a chemokine gradient CCL19 and CCL21. Integrin are family of αβ heterodimeric transmembrane cell surface proteins that are important in proper immune function (72).

The adaptive immunity to Mtb is to a large extent CD4+ T cell dependent (73). In addition, compelling results gathered from patients co-infected with TB and HIV have also underscored the critical role of CD4+ T cells in Mtb infection. This is because, the extent to which CD4+ T cell are depleted during acquired immunodeficiency syndrome disease correlated with increased susceptibility to primary infection as well as reactivation of latent Mtb infection (74) but, other adaptive immune-effector responses such as B cells and CD8+ T cells might also play a role (Haug et al. 2013).

1.2.3 The role of CD4+ T cells in mycobacterial infection

The effector subsets of CD4+ T cells is made up of Th1, Th2, Th17, T reg and Tfh cells (**1.1.7**). The ability of the immune system to control Mtb greatly depends on the development of Th1 responses consisting of IFN-γ and TNF-α secreting lymphocytes, which activates infected macrophages to induce antimicrobial activities (76). The proliferation of Mtb-specific CD4+ T cells occurs first in the draining lymph node (**1.2.2**). After activation, Mtb-specific CD4+ T cells then migrate into infected sites and produce IFN-γ, which is required for host survival (77). Genetic loss-of-function mutation in either IFN-γ or IFN-γ receptor in humans caused an increased susceptibility to Mtb (78). Also, mice which lack IFN-γ fail to control Mtb and succumb to TB within weeks of challenge (79, 80).

Furthermore, TNF produced by CD4+ T cells was also observed to be important in host defense against Mtb. This observation was made in animals which were treated with anti-TNF neutralizing antibody, lacked TNF gene, or genetically engineered to overexpress soluble TNF receptor. These animal models showed increased susceptibility to granulomatous pathogens such as Mtb and *Listeria monocytogenes*, as well as attenuated organisms such as *M. bovis* bacille Calmette-Guerin. (77, 81).

1.2.4 The role of autophagy in mycobacterial infection

The adaptive immunity to Mtb is to a large extent CD4+T cell dependent (**1.2.3**) and cytokines produced by Th1 and Th2 cells may have differential modulatory activity on autophagy as autophagy is stimulated by Th1 cytokines whereas Th2 cytokines suppress it (66, 82). A strong Th1 response, which is characterized by IFN-γ secretion is needed in defense against Mtb infection. IFN-γ has been found to induce autophagy in human and murine macrophage cell lines thus suppressing survival of virulent Mtb (83). Also, IFN-γ increases the proteolytic breakdown of long-lived proteins and translocation of LC3II into the isolation membrane (phagophore) leading to autophagosome formation (84). It was also demonstrated that mycobacteria-specific CD4+ T cells restored mycobacteria-inhibited autophagy in macrophages through cell-cell contact (67). The precise mechanism is yet to be fully elucidated, but immunity-related GTPases (Irgm1) have been shown to be involved (66).

The outlined literatures suggest that autophagy may be an important effector mechanism that might control the growth of mycobacteria in phagocytic cells. Furthermore, one of the main features of an immune response to Mtb is granuloma formation (**1.2.1**). Indeed, research has shown that the granuloma is severely hypoxic with ~0.2 % O_2 (85). Hypoxia induces the stabilization of HIF-1α, a transcription factor that is believed to be a central regulator of cellular survival in response to hypoxia. HIF-1α is responsible for inducing the expression of genes which are well suited for adapting to hypoxic conditions (61). It was also shown that hypoxia induces autophagy and this hypoxia-inducible autophagy was mediated by HIF-1α (86). This observation was made in numerous cell lines including mouse embryonic fibroblasts, under moderate and severe hypoxic condition. In peripheral T cells, HIF-1α protein synthesis is increased upon TCR engagement under hypoxia (87) and HIF-1α signaling was shown to suppress activation-induced T cell death

mediated by TCR stimulation (88). Thus, HIF-1α signaling enhances the survival of peripheral T cells. Furthermore, Th1 cells at the site of persistent phagosomal infections that result in granuloma formation acquire the ability to produce anti-inflammatory cytokine IL-10 (89). In addition, signaling through IL-10 receptor suppresses the IFN-γ and TNF-α production in CD4+ T cells (90, 91). Also, IFN-γ production by antigen-specific CD4+ T cells in granuloma-associated infections was shown to deteriorate progressively over time (89). Early production of IL-10 during T cell priming phase negatively affected antigen-specific CD4+ T cell expansion, maintenance and function in this study. Further, it is also known that IL-10 signaling inhibits autophagy (83, 92).
Taking together, these studies raise the question of how autophagy will be regulated in granuloma associated antigen (*Mycobacterium*)-specific-CD4+ T cells and does this impact T cell effector functions such as cytokine-production? Induction of autophagy seems necessary for cytokine production (22), proliferation, survival, memory formation and differentiation (93) of T cells. In order to unravel how mycobacteria-specific CD4+ T cells regulate autophagy and cytokine responses for example in response to presented antigen in the granuloma, novel assays which directly allow to measure autophagy in different subsets of mycobacteria-specific CD4+ T cells would in no doubt be imperative. The specific CD4+ effector T cell response to infection can be characterized by the cytokine profile produced in response to stimulation with antigen. The key to the study of autophagy in antigen-specific CD4+ T cells is therefore to quantify autophagy in parallel to specific effector cytokine production. This assay would play valuable roles in understanding the interplay of autophagy on the effector function of mycobacteria-specific CD4+ T cells and could be used to study for example the effect of hypoxia on CD4+ T cells as they appear *in vivo* in the granuloma of TB patients.

2 Aims and Objectives

The overall aim was:

To study autophagy in combination with effector cytokine production in mycobacteria-specific CD4+ T cells under hypoxic conditions.

However, in an effort to achieve this aim, the objectives for this study were:

- To establish and validate a flow-cytometric assay to study autophagy in primary human CD4+ T cells
- To polyclonally induce autophagy in primary human CD4+ T cells via TCR stimulation and study different aspects of T cell activation on autophagy
- To combine the flow-cytometric autophagy assay with additional extra- and intra-cellular staining with fluorescent antibodies to:
    - Quantify autophagy in different subsets of activated primary human CD4+ T cells
    - Quantify autophagy in activated effector cytokine producing CD4+ T cells under normoxic and hypoxic conditions
- To expand mycobacteria-specific CD4+ T cells from healthy donors to study autophagy and effector cytokine production in primary human antigen-specific CD4+ T cells.

3 Materials and Method (s)

3.1 Isolation of cells and mycobacteria-specific CD4+ T cell expansion

3.1.1 Isolation of Peripheral Blood Mononuclear cells (PBMCs)

Buffy coats were obtained from the blood bank of St Olav's Hospital, Norway. Ethical approval for the use of PBMCs isolated from blood donated by healthy donors for research purposes were obtained from the regional committee for Medical and Health Research Ethics at NTNU.

Isolation of PBMCs from buffy coats were carried-out using Lymphoprep (Axis-shield, Norway). The isolation protocol is based on density gradient centrifugation. Lymphoprep is a density gradient medium, which aids in separating mononuclear leukocytes (monocytes and lympohocytes) from erythrocytes and polymorphonuclear leukocytes (granulocytes) during centrifugation. Monocytes and lymphocytes have a lower buoyant density than erythrocytes and polymorphonuclear leukocytes (granulocytes). A large proportion of mononuclear cells have densities below 1.077 g/mL; hence they can be isolated by centrifugation on an isoosmotic medium with a density of 1.077 g/mL. This allows the erythrocytes and the polymorphonuclear leukocytes to sediment through the medium while retaining the mononuclear cells at the interface between the sample and the medium (Axis-shield density gradient media leaflet).

All reagents used in the isolation protocol were warmed to 37 °C and the isolation process was carried out in a laminar flow biosafety cabinet. The buffy coat was diluted with 100 mL sterile Dulbecco's phosphate buffer saline (DPBS; Sigma Aldrich, USA) in a sterile T75 culture flask and then aliquoted onto 14 mL Lymphoprep in a 50 mL Falcon tube. The diluted buffy coat was layered gently and slowly onto the Lymphoprep. This was done to prevent the blood from mixing with the Lymphoprep, which is toxic to blood cells. After layering, the tubes were centrifuged at 800xg for 20 min at 20 °C. The white layer obtained in the interface of the Lymphoprep and plasma was pipetted out into fresh tubes and then centrifuged at 950xg for 10 min, in order to get rid of blood components with lower densities compared to mononuclear cells. The supernatant was discarded and the pelleted cells were washed with 20 mL of Hanks' balanced salt solution (HBSS; Sigma Aldrich, USA) (by centrifuging at 150xg for 8 min) thrice. This procedure was employed

to get rid of blood components with higher density compared to mononuclear cells. The cells were then resuspended in Roswell Park Memorial Institute (RPMI)-1640 media supplemented with glutamine, HEPES and 10 % human serum matching the donors' blood group (hereafter referred to as RPMI-complete media). The cells concentration was then estimated by using Countess Automated Cell Counter (Invitrogen, Life technologies, USA). Counting was done by mixing 10 µl each of cell suspension and trypan blue (0.4 %) (Life technologies, USA). Finally, the concentration of cells needed for subsequent protocols were made.

3.1.2 Isolation of CD4+ T cells

CD4+ T cells were negatively isolated using MACS human CD4+ isolation kit (Miltenyi Biotec, Germany). The protocol is based on depletion of non-targeted (non-CD4+ T cells) cells in PBMCs enabling the isolation of highly purified CD4+ T cells. The kit consists of a cocktail of monoclonal antibodies conjugated to biotin (CD4+ T cell Biotin antibody cocktail) and a CD4+ T cell MicroBead cocktail. Non-CD4+ cells are labelled with the biotin-conjugated antibody cocktail and CD4+ T cell MicroBead cocktail. The magnetically labelled non-CD4+ T cells are depleted by retaining them on a MACS Column in a magnetic field of a MACS separator, while the unlabeled CD4+ T cells migrate through the column. In this study, MACS LS column and MidiMACS separator were used (**Appendix I**) (Miltenyi human CD4+ isolation kit data sheet).

The percentage of CD4+ T cells in PBMCs ranges from 25-60 % (Sanguine Bioscience Blog) and the yield of isolated CD4+ T cells from PBMCs is usually around 40 %. PBMCs number was chosen according to the number of CD4+ T cells necessary for each individual experiment. The following description is for 10 x 10^6 PBMCs and was scaled up accordingly for higher numbers of PBMCs used. The number of isolated PBMCs (**3.1**) desired for CD4+ T cell isolation was centrifuged at 600xg for 6 min and the supernatant was aspirated completely. The pellet was resuspended in 40 µl of buffer [consisting of DPBS + 0.5 % Fetal Calf Serum (FCS) + 2 mM ethylenediaminetetraacetic acid (EDTA)], followed by the addition of 10 µL of CD4+ T cell Biotin-Antibody cocktail. Cell and antibody were mixed thoroughly and incubated for 5 min on ice before 30 µL of DBPS + 0.5 % FCS + 2mM EDTA was added. Furthermore, 20 µL of the CD4+ T cell MicroBead cocktail was added, mixed thoroughly and gently, and incubated for an

additional 10 min on ice. Cells were kept cold and pre-cooled solutions were used in the isolation steps in order to prevent capping of antibodies on the cell surface and non-specific cell labeling.

MACS LS column was then placed in a magnetic field of MidiMACS separator and then rinsed with 3 mL of DBPS + 0.5 % FCS + 2 mM EDTA. The cell suspension was aliquoted onto the column and the flow through was collected, followed by rinsing the column with 3 mL of DBPS + 0.5 % FCS + 2 mM EDTA in order to flush out unlabeled cells from the column. The cells were counted and resuspended in the appropriate medium for downstream protocol.

3.1.3 Isolation of monocytes from PBMCs

Monocytes were isolated from PBMCs by plastic adherence due to the inherent property of monocytes to adhere to plastic (94). In this regard, isolated PBMCs were brought to a concentration of 10^7 cell/mL and 500 µL/well was aliquoted onto a 24 well plate. Likewise, for 96 well plates PBMCs were brought to a concentration of $2x10^7$ cell/mL and 100 µL were aliquoted into each well. The plates were then incubated for 1 h in the presence of 5 % carbon dioxide (CO_2) at 37 ^{0}C. After the incubation period, the non-adherent cells were washed three times with pre-warmed (at 37 ^{0}C) HBSS. Monocytes usually make up approximately 10 % of total PBMCs. Therefore, adherent monocytes in each well were estimated to be 5×10^5 cells (in 24 well plate) and 2×10^5 cells (in 96 well plate). 500 µL (24 well plate) and 200 µL (96 well plate) of RPMI-complete media were added to each well and the monocytes were rested overnight in the incubator for infection with *Mycobacterium avium* (*M. avium*) (24 well plate) or differentiation into monocyte-derived macrophages (96 well plate) as described in **3.1.6**.

3.1.4 Heat killing *M. avium*

The *M. avium* strain 104 expressing firefly luciferase was aliquoted into 10 mL of Middlebrook 7H9 medium in 50 mL Falcon tubes. The bacteria was then cultured in a shaker at 37 °C for 1-2 days. Optical density (OD) was checked using spectrophotometer set to 600 nm wavelength to ensure the bacteria was between 0.3 and 0.6 which indicate growth in the early log phase. An aliquot (1 mL) of the bacteria suspension was pelleted and then washed with DPBS at 10000xg for

2 min, followed by resuspension in 1 mL of DPBS. Further, the bacteria suspension was sonicated (30 s) three times, vortexing in-between. This was to disrupt bacteria aggregates. Optical density was measured and used in estimating the bacteria concentration (1 OD=450x10^6 CFU/mL). The bacteria suspension was placed in a heating block set to 70 ^{0}C overnight to kill the bacteria.

3.1.5 Expansion of mycobacteria-specific CD4+ Tcells

The expansion of *M. avium*-specific CD4+ T cells was performed using two different media during the culturing process. These two media are TexMACS medium, research grade (Miltenyi Biotec, Germany) and RPMI-complete media. TexMACS medium is an optimized serum-free cell culture medium, which is developed for the cultivation and expansion of human and mouse T cells. The medium was designed for optimal T cell growth, high cell viability, and consistency under serum-free conditions. It is produced without animal-derived components but contains pre-selected human serum albumin, stable glutamine and phenol red (Miltenyi Biotec TexMACS medium, research grade data sheet)

Isolated monocytes on a 24 well plate were infected 2 h with heat-killed *M. avium* at an MOI (multiplicity of infection) of 3. The plates were then washed twice with pre-warmed HBSS and 500 µL of the culturing media (TexMACS or RPMI-complete media) was added to each well. The infected monocytes were co-cultured with the isolated CD4+ T cells at 10^6 cells/mL for 13 days. After six days of culturing, 20 U/mL of recombinant human IL-2 (R&D Biosystems, USA) was added to each well. The cells were then harvested and pelleted (600xg for 6 min) after the expansion period. The pelleted cells from each media were counted after resuspending them in RPMI complete media for re-stimulation with autologous monocyte-derived macrophages (**3.1.6**).

3.1.6 Differentiation of monocyte-derived macrophages (MDMs)

Autologous monocyte-derived macrophages were generated as antigen-presenting cells from the same donor from which mycobacteria-specific CD4+ T cells were expanded (**3.1.5**). The isolated adherent monocytes (**3.1.3**) were differentiated with macrophage colony-stimulating factor (M-CSF) at a concentration of 50 pg/mL in RPMI-complete media. On the fourth day of incubation, half of the media was replaced with a fresh medium containing the same concentration of M-CSF. After 6 days, the cells were phenotypically differentiated into macrophages as observed under the light microscope. The macrophages were maintained healthy (by replacing half of the media every 3 days with RPMI-complete media without M-CSF) during the rest of the period while mycobacteria-specific CD4+ T cells were expanded.

3.1.7 Re-stimulation of mycobacteria-specific CD4+ T cells

Expanded *Mycobacteria*-specific CD4+ T cells (**3.1.5**) were re-stimulated on day 13 of expansion with the in parallel generated autologous macrophages (**3.1.6**). Autologous macrophages were stimulated overnight with heat killed *M. avium* at an MOI of 1 and 10 prior to addition of expanded CD4+ T cells. Expanded CD4+ T cells were added at a concentration of $5x10^5$ cells/mL into each well of infected MDMs on a 96 well plate. As a negative control, the expanded CD4+ T cells were co-cultured with uninfected macrophages. On the other hand, suspension of the expanded CD4+ T cells were stimulated with cell stimulation cocktail (500X) (eBiosciences, USA), at 1X concentration, which serves as a positive control. The cell stimulation cocktail consists of Phorbol 12-Myristate 13-Acetate (PMA) and ionomycin.

Treatment with PMA and ionomycin induces activation of many cell types to produce cytokines for detection in immunoassays. PMA is structurally analogous to DAG. It specifically activates PKC leading to NF-kB activation, by associating with the C1 domain of PKC. Ionomycin is a Ca^{2+} ionophore, which activates Ca^{2+}/calmodulin dependent signaling pathway leading to NFAT signaling. Ionomycin is also known to synergize with PMA in activating PKC signaling pathway (95, 96).

The co-cultured cells were incubated at 37 °C in 5 % CO_2 for 24 h. Protein transport inhibitor cocktail (eBioscience, USA) was added to all samples for the last 3-4 h. The protein transport inhibitor cocktail contains Brefeldin A and Monensin. These inhibit intracellular protein secretary pathways, leading to the accumulation of secreted proteins in the lumen of ER and Golgi apparatus. Consequently, this allows for intracellular cytokine staining. The treated cells were harvested into flow tubes and washed with DPBS supplemented with 2 % FCS for phenotypic characterization (**3.2.2**).

3.2 Characterization of CD4+ T cells

3.2.1 Flow-cytometry

The flow-cytometer is an instrument used in analyzing multiple characteristic of single cells. The key to flow cytometry is the analyses of cells in suspension. The process involves the interrogation of single cells (or other particles) as they flow through a beam of monochromatic light. By this method, the expression of intracellular or surface markers of cells can be analyzed. There are four fundamental components of a flow cytometer. These are the flow cell (chamber) that forces single cells into the middle of a fluidic sheath, a laser source of light, an optical component to focus light of different wavelengths onto a detector and a photomultiplier to amplify the signals (97, 98).

In a basic flow cytometer, the sample in suspension is drawn up into the flow chamber (cell) which lies at the heart of the flow cytometer. The flow chamber is designed to deliver cells in single file at the point of measurement. The cells flow rapidly and singly through the flow chamber and are interrogated by one or more beams of monochromatic light. Hydrodynamic focusing induces cells to orient with their long axis parallel to the flow. This allows the samples to pass by the laser beam with each cell oriented in the center of the sample stream (97).

The instrument operates on the laws of optics. Optics are present on the emission and excitation side. Excitation optics consists of the laser and lenses that focus the laser beam, and the emission optics are responsible for collecting the emitted light. As the laser beam hits the cell, the beam of light is scattered in a forward direction and a side direction. The scattered light and/or fluorescence (if fluorescent molecules are present on the cell) emission is then captured, filtered (wavelength

based), and channeled to the appropriate photodetectors or photomultiplier tube (PMT) for conversion to electrical signals (**Figure 3.1**). PMT functions by converting light into an electrical signal and amplifying the signal to a useful level by emitting secondary electrons. The signals are then amplified by the electronics in the cytometer and convert the analog data to digital data, which can then be analyzed by computer software programs (97).

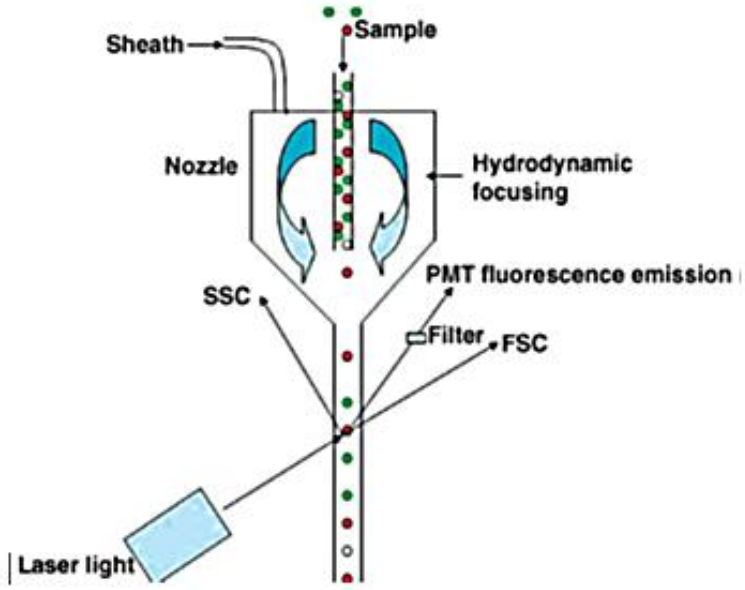

Figure 3.1: A diagrammatic representation of a flow-cytometer
Samples (fluorescently labeled) are hydrodynamically focused singly in the flow cell. Each cell is excited by a laser light and the emissions (FSC and SSC) are detected. The diagram above has been adapted from (97)

Due to different refractive indices between the cells and the sheath fluid, incident lights on cells are scattered in the forward and side directions. This gives empirical data about the physical characteristics of the cell (**Figure 3.1**). Light scattered in the forward direction is detected by forward scatter channel (FSC) and it measures the cell size whereas light scattered at 90 degrees to the laser path are detected by the side scatter channel (SSC) and measures the granularity of the cell.

The flow-cytometer uses multiple lasers that are spatially positioned such that there is a sequential time delay for each laser beam that intercept with the cells. Fluorochrome-tagged antibodies are

used to label specific markers on cells which can then be excited with a particular wavelength of light from the laser. Fluorochromes are molecules that absorb light at specific wavelength causing electrons to excite to a higher energy level. When the electron returns to the ground state, they emit a quantum of energy (**Figure 3.2**). The process is referred to as fluorescence.

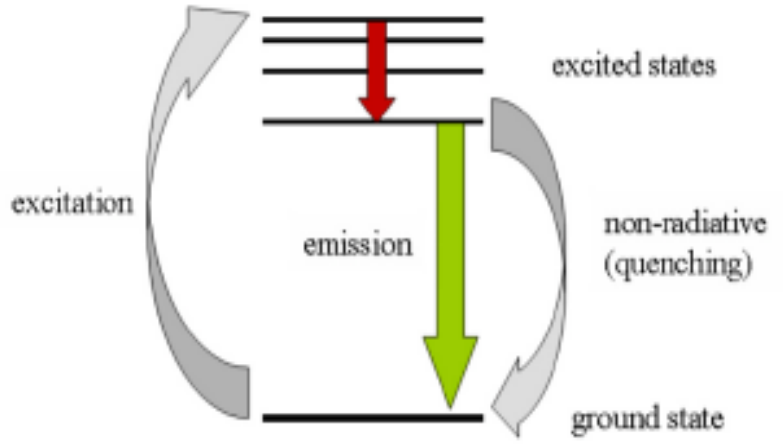

Figure 3.2: A schematic representation of absorption and emission of light during fluorescence The electrons in fluorochromes get excited by absorbing light and then move to a higher energy state (excited state). The electrons then return to the ground state emitting quantum of energy. The figure was culled from (99).

All emitted signals from fluorochromes are routed to detectors by a system of mirrors and optical filters. The filters used are the short-pass filter, long-pass filter and the band-pass filter. The short-pass filter transmits light wavelength equal to or shorter than the specified wavelength, long-pass filters transmit light wavelength equal to or longer than the specified wavelength and band-pass filters allow a narrow range of wavelength to reach the detector. The choice of filters optimizes detection of the specific fluorochrome by one detector or photomultiplier tube (PMT), since each fluorochrome has a specific emission spectrum. The detection of fluorescence requires selection of appropriate filters that are placed before each detector or PMT. The type of filter selected must collect as much emitted light from the primary fluorochrome for high sensitivity, but as little as possible from other fluorochromes to reduce the compensation required (97, 100).

Fluorochromes can contribute signals to several detector due to spectral overlap (**Figure 3.3**) therefore, multicolor flow-cytometry faces the problem of fluorescent spillover. The contribution

of signals in detectors not assigned to a fluorochrome must be removed from the total signals in those detectors. This process is popularly referred to as compensation (97, 101).

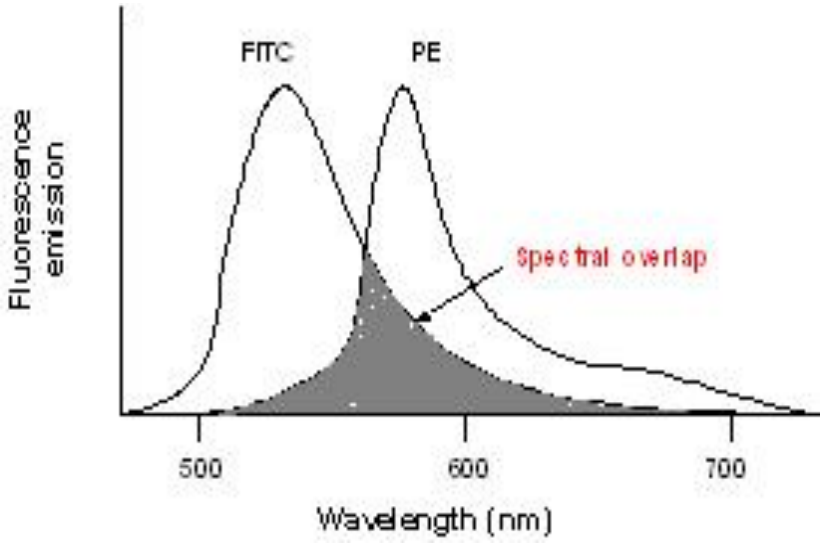

Figure 3.3: Schematic representation of spectral overlap between fluorescein isothiocyanate (FITC) and phycoerythrin (PE) fluorochromes after excitation.
(Figure from AppliedCytometry)

In this study, compensation was carried out using compensation beads (BD Biosciences, USA). This was done for all the fluorochromes used in the study and involves singly stained compensation beads with fluorochrome labelled antibodies. After analyzing the compensation bead samples, compensation in each channel was automatically calculated by the FACS Diva (BD Biosciences) software. The flow cytometer (BD LSR II) used for this project is equipped with 4 lasers and several filter combinations.

3.2.2 Phenotyping CD4+ T cells

Expanded mycobacteria-specific CD4+ T cells or polyclonally activated CD4+ T cells were extra- and intra-cellularly stained with fluorescent antibodies for analysis by flow-cytometry. Antibodies used for extracellular labelling CD4+ T cell surface antigens were anti-CD3, anti-CD4, anti-CD25, anti-CD69 and anti-CD40L monoclonal antibodies conjugated to brilliant violet (BV) 785, BV711,

BV510, PE and BV605 respectively. Antibodies used in this project were titrated after cells were polyclonally activated with plate bound aCD3/aCD28 (**3.3.2**). The stock concentration of all antibodies used in this study differed, however 1 µL of each antibody stock was appropriate for CD4+ T cells phenotyping (Data not shown).

In order to facilitate accurate pipetting, all antibodies required to stain surface epitopes of the cells were pooled together by aliquoting 1 µL each per sample and then made-up to a final volume of 10 µL for each sample by adding DPBS supplemented with 2 % FCS. After aliquoting 10 µL of the pooled antibodies unto each sample, they were vortexed and incubated for 20 min in the dark on ice. The cells were then washed (600xg for 5 min) to remove unbound antibodies and resuspended in 500 µL of fixable viability dye eFluor 780 (eBiosciences, USA) for 30 min on ice in the dark. The cells were washed and resuspended (500 µL) in 2 % paraformaldehyde (PFA) for 20 min at room temperature in order to fix the cells. PFA acts by intra- and inter-molecular cross-linking amino acids (102) thereby preserving the state of the cell prior to permeabilization with saponin. After PFA treatment, the cells were washed (600xg for 5 min) and resuspended in 500 µL permeabilization buffer (0.5% saponin + 1 % FCS in DPBS) for 5 min at room temperature, followed by pelleting the cells. Subsequently cells were intracellularly stained with fluorescent labeled anti-IFN-γ, anti-TNF-α and anti-IL-2 monoclonal antibodies conjugated to allophycocyanin (APC), BV421 and phycoerythrin/Cyanine 7 (PE/Cy7). Again, to ensure accurate pipetting the antibodies were pooled as described previously and permeabilization buffer was added to make up 10 µL for each sample. 10 µL of the pooled antibodies were added to each sample, vortex and incubated in the dark at room temperature for 30 min, after which they were washed (600xg for 5 min) twice. Data were then collected using FACSDiva software on the LSR II flow-cytometer by acquiring 50000 events per sample. Data were subsequently analyzed by FlowJo analysis software (Treestar Inc., USA).

3.3 Autophagy in CD4+ T cells

3.3.1 Polyclonal activation of CD4+ T cells

CD4+ T cells were activated with the aim of inducing autophagy, using phytohemmaglutinin (PHA), concanavalin (Con) A, and anti-CD3 conjugated plates plus soluble anti-CD28. All of

these agents polyclonally activate T cells. PHA and Con A are lectins derived from plant origin. Lectins are proteins that interact with specific sugar residues. PHA is isolated from red kidney bean, *Phaseolus vulgaris* and Con A is isolated from Jack beans, *Canavalia ensiformis.* These lectins are able to induce blastogenesis *in vitro*, in various forms of mammalian mononuclear cells.

Anti-CD3 conjugated plates are used to activate T cells and consists of functional grade anti-human-CD3 (clone OKT3) and -CD28 (clone CD28.2) antibodies (eBiosciences, USA). The anti-CD3 was immobilized onto a polystyrene plate and engaged the invariant signaling component of the TCR. The anti-CD28 was then added to induce full T cell activation, mimicking physiological T cell activation by providing co-stimulatory signal.

Anti-CD3 (8 µg/mL) was prepared and 50 µL was dispensed onto a 96 well plate. The plate was tightly covered with parafilm and incubated at 37 °C for 2 h. The parafilm was used in order to prevent sample evaporation. After the incubation period, each well was washed with 200 µL of sterile DPBS twice to remove unbound antibodies. Isolated CD4+ T cells (**3.1.2**) were brought to a concentration of $1x10^6$ cell/mL and 200 µL was aliquoted into each well. Anti-CD28 antibodies were then added to each well at a final concentration of 2 µg/mL. For stimulation of CD4+ T cells with PHA and Con A, 200 µL of the $1x10^6$ cell/mL CD4+ T cells were cultured in the presence of 2.5 µg/ml (PHA) and 10 µg/mL (Con A). Cells were cultured in an incubator (37 ^{0}C + 5 % CO_2) under normoxic (ca. 20 % O_2) or hypoxic (2 % O_2) conditions for 24 h, 48 h and 72 h in the presence or absence of chloroquine (10 µM) for the last 18 h.

3.3.2 IFN-γ Secretion Assay

The IFN-γ Secretion Assay - Cell Enrichment and Detection kit (Miltenyi, Germany) is designed for the detection, isolation and analysis of viable IFN-γ producing leukocytes. IFN-γ is predominantly secreted by CD4+ and CD8+ effector and memory T cells and NK cells upon activation. After specific antigen stimulation of CD4+ T cells *in vitro* IFN-γ production is induced in antigen-specific T cells which can be isolated by the kit. Staining of IFN-γ secreting cells with the kit was performed according to the manufacturer's recommendations (IFN-γ secretion Assay data sheet). The principle is based on the attachment of IFN-γ Catch Reagent to the cell surface of leukocytes. The cells are then incubated for a short period of time at 37 °C to allow cytokine

secretion. The secreted IFN-γ binds to the IFN-γ Catch Reagent on the positive, secreting cells, which are then subsequently labeled with IFN-γ detection antibody conjugated to PE for sensitive detection by flow-cytometry. (IFN Secretion assay-cell Enrichment and Detection kit data sheet).

For the experiments in this study, isolated CD4+ T cells (15 x 10^4 cells/well) were stimulated with plate bound aCD3/aCD28 for 48 h in the presence and absence of chloroquine for the last 18 h. After stimulation, the cells were washed with 10 mL cold buffer (DPBS + 0.5 % FCS + 2mM EDTA), centrifuged at 650xg for 5 min at 5 °C. The supernatant was pipetted off completely and cells were resuspended in 80 µL of cold RPMI-complete medium, after which 20 µL of IFN-γ Catch Reagent was added, mixed well and incubated on ice for 5 min. The cells were then diluted with 20 mL of warm RPMI-complete media and incubated in a closed 50 mL Falcon tube under gentle rotation at 37 °C using the MACSmix tube rotator for 45 min. After incubation, cells were placed on ice and the tube was filled with cold DPBS + 0.5 % FCS + 2mM EDTA and centrifuged at 650xg for 5 min at 5 °C. The supernatant was pipetted off completely and 80 µL of cold DPBS + 0.5 % FCS + 2mM EDTA and 20 µL of IFN-γ detection antibody was added and cells were gently resuspended. The cells were placed on ice for 10 min and later washed by adding 10 mL of cold buffer. The supernatant was pipetted off completely and the cells were stained with CytoID dye as described in **3.3.3** and then phenotyped as in **3.2.2**.

3.3.3 Detection of autophagy using CytoID autophagy detection kit

CytoID Autophagy detection kit (Enzolifesciences) measures autophagy in live cells by using a novel dye, a cationic amphiphilic tracer dye that partitions into cells in a way similar to phospholipidosis-inducing drugs. According to the manufacturer, the dye has been optimized through a careful selection of titratable functional moieties that allows for minimal staining of lysosomes while exhibiting bright fluorescence upon incorporation into autophagosomes and autophagolysosome. This assay offers a rapid and quantitative approach in monitoring autophagy in live cells without the need for transfection (CytoID autophagy detection kit product manual).

Autophagy was induced in CD4+ T cells as described in **3.3.1**. Cells were harvested and washed with indicator free media (consisting of DPBS supplemented with 5 % FCS) at 600xg for 5 min.

The cells were then resuspended in 250 µL of the indicator free media. The CytoID stain (1000X) was diluted (1:1000) with 1X Assay Buffer and 250 µL of the diluted CytoID green dye solution was added to each sample and mixed well by gently pipetting up and down to achieve a mono-dispersed cell suspension. The samples were incubated for 30 min in the dark at room temperature after which the cells were collected by centrifugation and washed with 500 µL of 1X Assay buffer. The cells were then phenotypically characterized by flow-cytometer as described in **3.2.2.**

3.3.4 Autophagy detection by immunoblotting

Immunoblotting (Western) blotting is an important technique used in cell and molecular biology to help identify specific protein of interest from complex mixture of proteins extracted from cells. Three elements are used by the technique to accomplish this task: (1) separation by size, (2) transfer to a solid support and (3) marking targets using specific primary and secondary antibodies. To separate the proteins by size, the three-dimensional conformation of the protein is denatured by sodium dodecyl sulfate (SDS) and dithiothreitol (DTT), thus introducing a uniform negative charge along the protein. This allows the protein to migrate towards the anode during electrophoresis. The denatured proteins are loaded on polyacrylamide gel with defined pore sizes, which allows the proteins to migrate to different positions on the gel depending on their sizes. After sample separation, the proteins are transferred onto nitrocellulose membrane. Nitrocellulose binds proteins with a very high affinity. Protein transfer is done using an electric current perpendicular to the surface of the gel, causing the protein to migrate unto the membrane. The blot is blocked with Bovine Serum Albumin (BSA) and then incubated with specific antibodies against the protein of interest, followed by incubation with a labeled secondary antibody. This allows for visualization of specific bands of interest on the blot. The specific bands of interest are compared with standard ladder of known molecular weight to determine the size of the protein of interest (103). The autophagy protein analyzed is LC3 (**1.1.2**).

For the experiments in this study, isolated CD4+ T cells were stimulated with plate-bound aCD3/aCD28 for 24 h, 48 h, and 72 h in the presence and absence of Bafilomycin (BAF) A1 (100 nM) for the last 3 h. After treatment, the cells were collected by centrifugation (1100xg for 7 min at 4 °C) in an Eppendorf tube. Aliquots of 40 µL lysis buffer (**Appendix II**) was added to each tube and kept on ice. After adding the lysis buffer, each tube was vortex with intermittent

sonication three times to help lyse the cells. The supernatant was then collected by centrifugation at 9391xg for 20 min at 4 °C using the Eppendorf centrifuge. Aliquots of 20 µL protein lysate were mixed with 10 µL of NuPage LDS loading buffer 4X containing 0.1M DTT (Invitrogen, USA). The tubes were then placed on heating block set to 70 °C for 10 min to denature the protein. The mixture was loaded (28 µL) unto the 10 % NuPage Novex Bis-Tris Gel along with 7 µL of SeeBlue marker (Life technologies, USA) and 1 µL of Magic marker (Life technologies, USA) in the first and the last wells. The gel was then run with NuPAGE MES SDS running buffer using the following settings: 30 min at 100V and then 90 min at 150V. The gel was then transferred unto the nitrocellulose membrane using the iblot dry blotting system for 10 min after which the membrane was washed with Tris Buffered saline with Tween-20 (TBS-T) (**Appendix II**) under agitation for 5 min. The membrane was then blocked with 5 % BSA in TBS-T under agitation for 1 h after which it was incubated overnight with the rabbit anti-LC3B (Cell signaling technologies, USA) primary antibody (diluted at the ratio of 1:1000 with 5 % BSA) under agitation. The membrane was washed 5 min with TBS-T thrice and then incubated with swine anti-rabbit immunoglobulin/HRP (Dako, Denmark) secondary antibody diluted with TBS-T at a ratio of 1:2000 for 1 h. The membrane was washed with TBS-T for three times and then developed with chemiluminesence SuperSignal West Femto maximum sensitivity substrate (Thermo Scientific, USA) for 5 min. After developing, the membrane was visualized with Odyssey Fc (LI-COR Biosciences, UK) on the chemiluminescent channel. To correct for concentration variation in each sample lane, detected proteins of interest were normalized to β-actin which is constitutively expressed in cells. The membrane was washed three times with TBS-T and incubated with mouse anti-actin (Sigma Aldrich, USA) (diluted with TBS-T at 1:5000) for 45 min under agitation. The membrane was washed with TBS-T thrice and then incubated with the goat anti-mouse immunoglobulin/HRP (Dako, Denmark) secondary antibody diluted in TBS-T at a ratio of 1:10000. The membrane was then developed with the SuperSignal West Femto maximum sensitivity substrate for 5 min and visualized under the chemiluminescent channel.

4 Results

In spite of the recent advances in understanding autophagic processes there are still limited experimental techniques that may be used to study autophagy. The methods commonly used in monitoring autophagy are electron microscopy, immunofluorescence by confocal microscopy, western blotting analysis of LC3 and Atg 8 turnover, and more recently flow-cytometry (104). There are currently no assays available to visualize autophagy directly in different subsets of CD4+ T cells such as cytokine-producing CD4+ effector T cells (e.g., mycobacteria-specific CD4+ T cells). In this project, methods were established and utilized to study autophagy in subsets of primary human CD4+ T cells from healthy donors by flow-cytometry using CytoID autophagy detection kit (Enzolifesciences). The kit consists of a cationic amphiphilic tracer dye which specifically stains autophagolysosomes and autophagosomes without the need for transfection. Flow cytometry has the unique ability to simultaneously measure and analyze multiple physical characteristics at a single cell level in a heterogeneous cell population.

4.1 Autophagy is induced in CD4+ T cells upon TCR stimulation

It has been suggested that TCR stimulation induces signaling pathways which results in upregulation of autophagy (22). Furthermore, it was previously demonstrated that CytoID kit could be used to specifically detect autophagy in CD4+ T cells by flow-cytometry (Master Student: Ibrahim, 2014). The starting point of this project was to replicate autophagy induction in primary human CD4+ T cells via TCR stimulation and quantify autophagy in them. For this purpose, the use of a flow-cytometric method would be advantageous since flow-cytometry measures in addition multiple physical parameters in a heterogeneous cell sample. In this study, the flow-cytometric method was further validated and subsequently used to study autophagy in different subsets of CD4+ T cells during activation, differentiation and effector cytokine production.

Full T cell activation requires three signals. Signal one involves signaling through the TCR whereas signal two occurs through costimulatory molecules such as CD28 and signal three comes from IL-2 and other priming cytokines. T cells produce and respond to IL-2, and IL-2 is produced in response to concerted CD28 and TCR stimulation. We thereby set-out to induce autophagy in

CD4+ T cell using different TCR stimulation reagents. To detect autophagy, primary CD4+ T cells were isolated from PBMCs by negative selection using human CD4+ isolation kit (**3.1.2**). The isolated CD4+ T cells were checked for purity by flow-cytometry and the purity of all isolated CD4+ T cells used in this project was ≥ 94 % (**Appendix III**).

The isolated CD4+ T cells were stimulated with the following reagents: plate bound anti-CD3 (aCD3) and anti-CD28 (aCD28), plate-bound anti-CD3 alone, phytohemagglutinin (PHA) and concanavalin A (Con A) (**3.3.1**). Anti-CD3 is an antibody to the invariant signaling molecule CD3, aCD28 is on the other hand an antibody which crosslinks the co-stimulatory molecule CD28, and PHA and Con A are plant lectins which are known to indirectly crosslink TCR. The stimulated cells were cultured for 24 h, 48 h and 72 h with or without chloroquine (CQ) (10 µM) for the last 18 h and then harvested for CytoID staining. CQ is a lysosomotropic drug which increases lysosomal pH, thereby inhibiting the activity of acidic lysosomal hydrolases resulting in the accumulation of autophagosomes (105). Thus, CQ inhibits autophagy flux. After CytoID staining, the cells were phenotypically characterized as described in materials and method (**3.2.2**). The characterized cells were analyzed by flow-cytometry and lymphocyte gates were defined in the FSC and SSC, followed by viability gate and gating for CD3+CD4+ T cells (**Figure 4.1a**). Overlays of histogram plots were then generated for CytoID dye from the CD3+CD4+ gated T cells and subsequently normalized to mode (**Figure 4.1b**). The histogram overlays in each plot is a comparison of cells treated with (bottom) and without (top) CQ over the stimulation period. There was a rightward shift of the histogram plots along the CytoID axis to 72 h stimulation (**Figure 4.1b**). This is suggestive of increasing autophagosome and autophagolysosome levels over the stimulation period, since CytoID is known to stain autophagosomes and autophagolysosomes (Enzolifescience). Also, comparing histogram overlays for cells treated with (bottom) and without (top) CQ, there was a moderate rightward shift from cells which were not CQ treated to cells treated with CQ for each time point along the CytoID axis (**Figure 4.1b**).

From the histogram plots (**Figure 4.1b**) CytoID median fluorescence intensity (MFI) was quantified for all time-points for the different stimulation reagents to generate a line plot (**Figure 4.1c, d**). There was an observed overall-increase in MFI over the stimulation period with all the stimulation reagents indicating an increased induction of autophagy. CQ inhibits autophagic flux and as expected cells treated with CQ showed higher MFI compared to cells which were not treated

with CQ (**Figure 4.1c, d**). Furthermore, CD4+ T cells stimulated with Con A showed higher MFI than PHA (**Figure 4.1d**) and those stimulated with plate bound aCD3/aCD28 on the other hand showed higher MFI than plate bound aCD3 alone (**Figure 4.1c**). However, comparing plate bound aCD3/aCD28 and aCD3 to Con A activated (stimulated) cells (**Figure 4.1c, d**), aCD3/aCD28 and aCD3 activated cells showed higher MFI. Relatively, there seems to be minimal differences (in MFI) between plate bound aCD3 and aCD3/aCD28 stimulated cells (**Figure 4.1c**), indicating that there is not much differences in the level of autophagy induced by TCR stimulation via signal one alone or signal one and two.

CytoID dye is a relatively new compound, which is used to study autophagy and the company only provided little information on the compound. Therefore, these initial results were confirmed by a second method. Classical and well established methods used to study autophagy include confocal microscopy and immunoblot analysis of LC3. LC3 is a prototypic marker for autophagy. During the induction of autophagy, LC3I is converted to the lipidated form LC3II, which is incorporated into the growing autophagosome and subsequently degraded in the autophagolysosome by lysosomal hydrolases (9). Quantification of LC3 abundance by immunoblotting was then chosen to confirm CytoID results obtained on autophagy-induction in CD4+ T cells. In this regard, isolated CD4+ T cells were stimulated with plate bound aCD3/aCD28 for 24 h, 48 h and 72 h with and without BAF A1 for the last 3 h of stimulation. BAF A1 is a lysosomal Na^+H^+ pump inhibitor, which inhibits lysosomal hydrolase activity leading to autophagosome accumulation (105). Cells were treated for immunoblotting as described in **3.3.4.** An increased accumulation of LC3II was observed over time in response to TCR stimulation with aCD3/aCD28 (**Figure 4.1e, f**). For each time point, as expected CD4+ T cells treated with BAF A1 showed an increased LC3II abundance compared to CD4+ T cells without BAF A1 treatment (**Figure 4.1e**). LC3II levels at each time point were quantified and normalized to actin, a housekeeping protein which is constitutively expressed in cells independent of TCR stimulation (**Figure 4.1f**). Normalized quantification at 48 h showed an 12-fold increase in LC3II abundance compared to 24 h and then an 54-fold increase at 72 h (**Figure 4.1f**). Results obtained from immunoblotting confirmed the findings of CytoID by flow-cytometry, thus encouraging us to trust CytoID as suitable tool to measure autophagy in T cells. In addition, CytoID findings were confirmed with LC3 II staining by confocal microscopy in another project in our group (Master Student: Ibrahim, 2014). Autophagy was therefore

analyzed in all the following experiments with CytoID by flow-cytometry as immunoblotting has the limitation of not easily allowing the analysis of further parameters or autophagy in cell subsets.

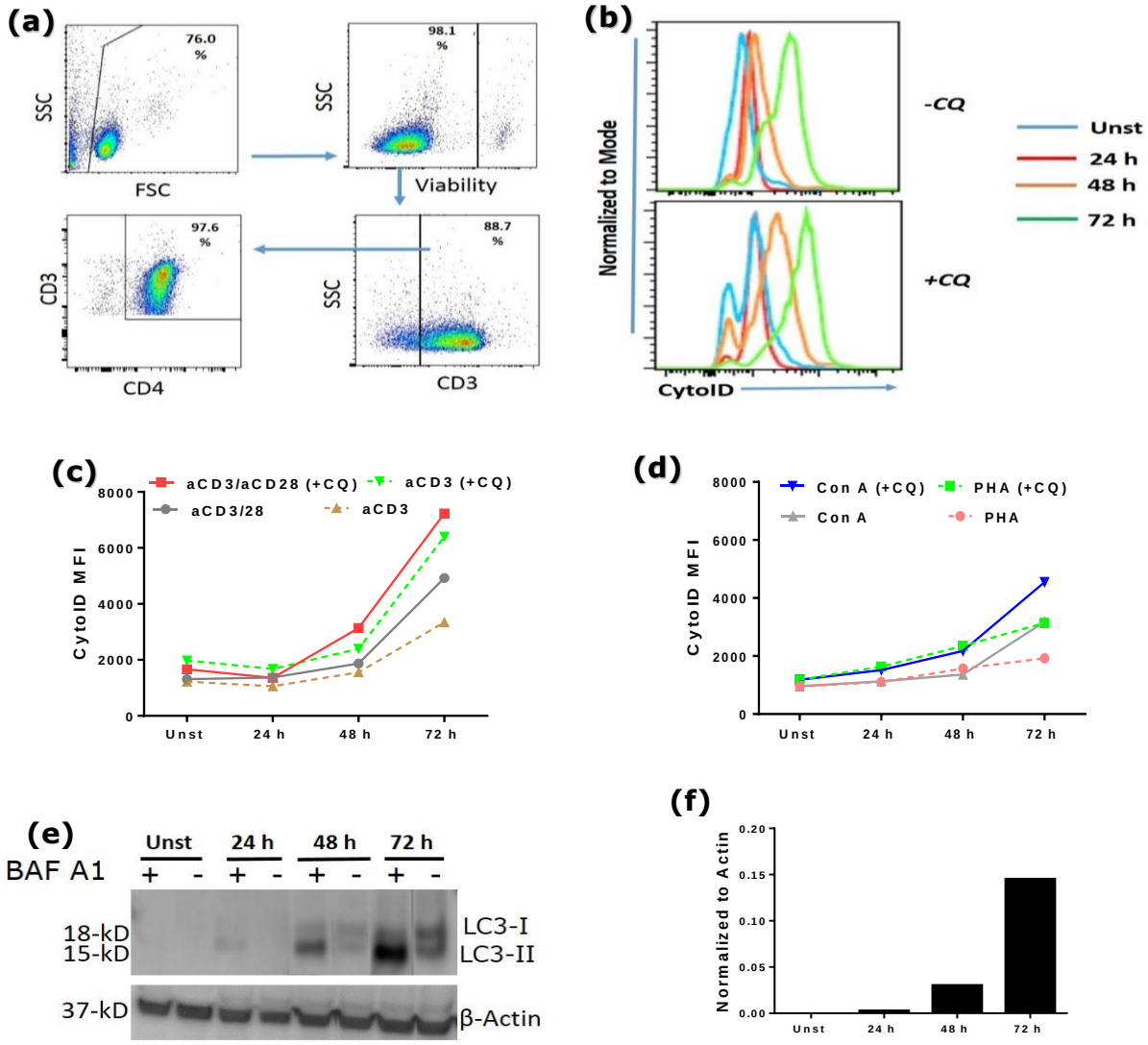

Figure 4.1: Increased autophagosome abundance in CD4+ T cells upon TCR stimulation.

(a) Example of gating strategy to identify viable CD4+ T cells. The lymphocyte gate was defined in the FSC and SSC, followed by viability, CD3+ gating and then CD3+CD4+ gate. The gates shown was for cells stimulated 24 h with aCD3/aCD28 **(b)** Overlays of histogram plots for CytoID treated cells from CD3+CD4+ gated T cells. The histogram plots are representative of cells stimulated with plate bound aCD3/aCD28 for 24 h, 48 h, and 72 h, which were then normalized to mode. The histogram overlay is a comparison of cells stimulated at different time points with CQ (bottom) and without CQ (top) treatment. **(c)** Quantified CytoID MFI of plate bound aCD3 (8 µg/mL) and aCD3/aCD28 (8 & 2 µg/mL respectively) stimulated CD4+ T cells with and without

CQ treatment over time. **(d)** Quantified CytoID MFI of Con A (10 µg/mL) and PHA (2.5 µg/mL) stimulated CD4+ T cells with and without CQ treatment over time. Data are representative of two different experiments with similar outcomes. **(e)** Immunoblot analysis of LC3 and actin at 24 h, 48 h and 72 h post stimulation of purified CD4+ T cells with plate bound aCD3/aCD28, in the presence or absence of BAF A1 for the last 3 h **(f)** Quantification of LC3II expression at the various time points of stimulation normalized to actin. The immunoblot analysis is representative of two experiments with similar findings.

4.2 Anti-CD28 and IL-2 without direct TCR stimulation did not induce autophagosome abundance in CD4+ Tcells

To further dissect the effect of the other signals (signals two and three) which are required for full T cell activation on induction of autophagy, there was an attempted induction of autophagy in CD4+ T cells using anti-CD28 and IL-2 alone without providing direct TCR signal via anti-CD3. Isolated CD4+ T cells were cultured in the presence of anti-CD28 (2 µg/mL) or IL-2 (2 U/mL, 20 U/mL and 100 U/mL) for 24 h, 48 h and 72 h with and without CQ treatment for the last 18 h. After each incubation period, cells were harvested and stain with CytoID dye as described in **3.3.3**. Data was collected and gates were defined as in **Figure 4.1a**, and then quantified for CytoID MFI to analyze autophagosome abundance. No change in autophagy level was observed for anti-CD28 and IL-2 treated cells (**Figure 4.2a, b**). As expected, CQ treated cells showed higher MFI compared to cells without CQ treatment (**Figure 4.2a, b**).

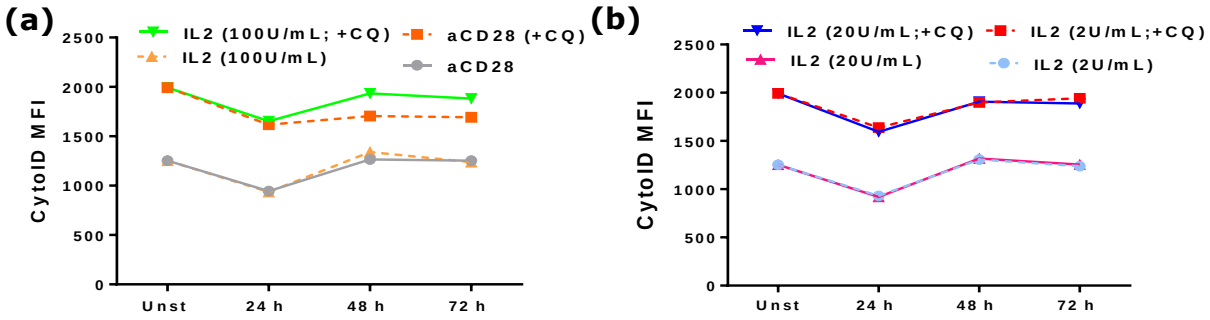

Figure 4.2: Basal levels of autophagy in anti-CD28 and IL-2 stimulated CD4+ T cells.

(a) CD4+ T cells treated with anti-CD28 (2ug/mL) and high dose of IL-2 (100U/mL) with and without CQ **(b)** CD4+ Tcells treated with IL-2 (low and medium doses) with and without CQ treatment. The experiment was repeated twice with similar findings.

4.3 Autophagy in CD4+ T cells could not be quantified with CytoID in combination with intracellular antibody-staining

After activation, CD4+ T cells differentiate into different effector CD4+ T cell subsets which can be distinguished by the cytokine profile they produce (**1.1.7**). The key to accurately and specifically study autophagy regulation in any specific T cells (e.g., mycobacteria-specific CD4+ T cells) is to quantify autophagy in specific cytokine producing cells. Quantifying autophagy in specific cytokine producing cells would be a very good representation of how autophagy is actually regulated in specific T cells. Preliminary results (**Figure 4.1**) showed that CytoID can be used to quantify autophagy in CD4+ T cells. To learn more about the effector function of activated CD4+ T cells and the importance of autophagy in antigen-specific CD4+ T cell subtype differentiation and function, it would be desirable to combine CytoID with intracellular effector cytokine staining (ICS). Therefore, we attempted the combination of CytoID staining in activated CD4+ T cells along with intracellular cytokine staining.

In order to pave way for combined CytoID stain and intracellular cytokine staining (ICS), the influence of various fixation and permeabilization buffers in CytoID channel (488nm laser) was assessed. In this regard, isolated CD4+ T cells were stimulated with plate bound aCD3/aCD28 for 48 h. The cells were harvested, fixed and then permeabilization with permeabilization buffers purchased from eBiosciences and R&Ds, and in-house made (2 % PFA and 0.5 % saponin) permeabilization buffer. Data was analyzed and overlay of histogram plots were generated using CytoID channel (**Appendix IV**) and CytoID MFI was subsequently quantified. The use of the in-house made fixation and permeabilization buffer resulted in an increased fluorescence signal (auto-fluorescence) in the CytoID channel. However, permeabilization buffers from R&Ds and eBiosciences showed minimal increase in auto-fluorescence with signals in the CytoID channel comparable to the negative control (cells with no treatment) (**Appendix IV**). Therefore, we continued and attempted the combination of CytoID staining along with ICS using R&Ds permeabilization buffer.

In this regard, isolated CD4+ T cells were stimulated for 48 h with and without CQ treatment for the last 18 h. The cells were CytoID stained with and without fixation and permeabilization. Data was collected, analyzed and an overlay of CytoID histogram plots was made (**Figure 4.3**). In

previous experiments autophagy was found to increase after 48 h of CD4+ T cell activation as measured by CytoID. However, treatment of activated CD4+ T cells with R&Ds permeabilization buffer after CytoID staining resulted in complete loss of CytoID intensity with fluorescent intensity comparable to unstimulated samples (**Figure 4.3**).

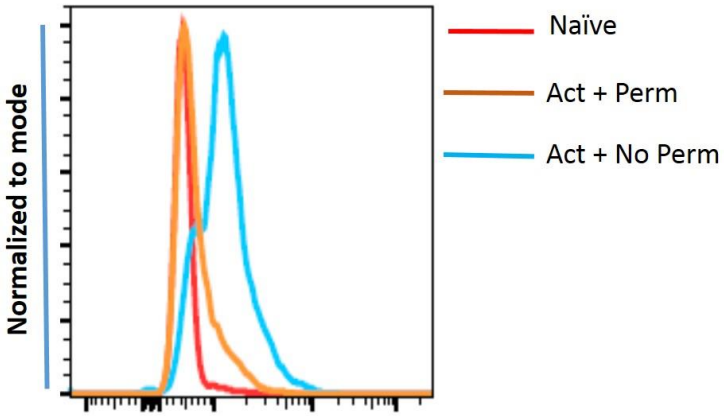

Figure 4.3: Fixation and permeabilization treatment after CytoID staining leads to loss of signal. The figure shows CytoID histogram overlay of naïve untreated (red) CD4+ T cells and CD4+ T cells activated 48h with aCD3/aCD28 without (blue) and with (orange) treatment with R&Ds fixation and permeabilization buffer after CyoID staining. This result is a representation of two different experiments with similar outcomes.

4.4 Expression of surface activation markers on CD4+ T cells is not affected if autophagy flux is inhibited by chloroquine

The attempted combination of ICS with CytoID has proven problematic (**Fig. 4.3**). Therefore, we set out next to analyze autophagy in combination with extracellular activation marker staining on CD4+ T cells, which are known to be expressed on the cell surface after TCR stimulation. As this does not require fixation and permeabilization procedures. The expression of activation markers CD25, CD40L and CD69 on the surface of activated CD4+ T cells were assessed in combination with CytoID autophagy measurement. However, to appropriately study autophagy, inhibition of autophagy flux is needed. In this regard, we first studied if autophagy flux inhibition using CQ may have an effects on the expression of surface activation markers.

In this regard, isolated CD4+ T cells were stimulated with plate bound aCD3 and aCD3/aCD28 in the presence or absence of autophagy flux inhibitor CQ for the last 18 h of CD4+ T cell culture. Cells were cultured for 24 h, 48 h and 72 h. Data was collected and gates were defined for CD3+CD4+ T cells (as in **Figure 4.1a**) and further analyzed for activation markers CD25, CD40L and CD69 expression (**Figure 4.4a**). There was a strong induction of CD69 upon stimulation after 24 h, which was sustained over 72 h (**Figure 4.4a, c**). CD40L was on the other hand weakly expressed over 48 h. We did not see clear differences in CD40L expression after 24 h and 48 h, but after 72 h there was about 16-fold increased expression of CD40L (**Figure 4.4a, d**). We observed moderate induction of CD25 expression after 24 h, which increased to 48 and 72 h (**Figure 4.4a, b**). The frequencies of activation marker CD40L, CD25 and CD69 showed no obvious differences between activated CD4+ T cells cultivated in the presence or absence of the autophagy flux inhibitor CQ over the stimulation period. These results suggest that autophagy flux inhibition does not affect CD25, CD69 and CD40L expression after CD4+ T cell activation. Minimal differences in activation marker CD40L and CD69 expression at each time point were observed between aCD3 and aCD3/aCD28 activated cells (**Figure 4.4 c, d**). Regarding CD25 expression, aCD3/aCD28 activated cells showed higher expression than aCD3 activated cells over the stimulation period (**Figure 4.4b**)

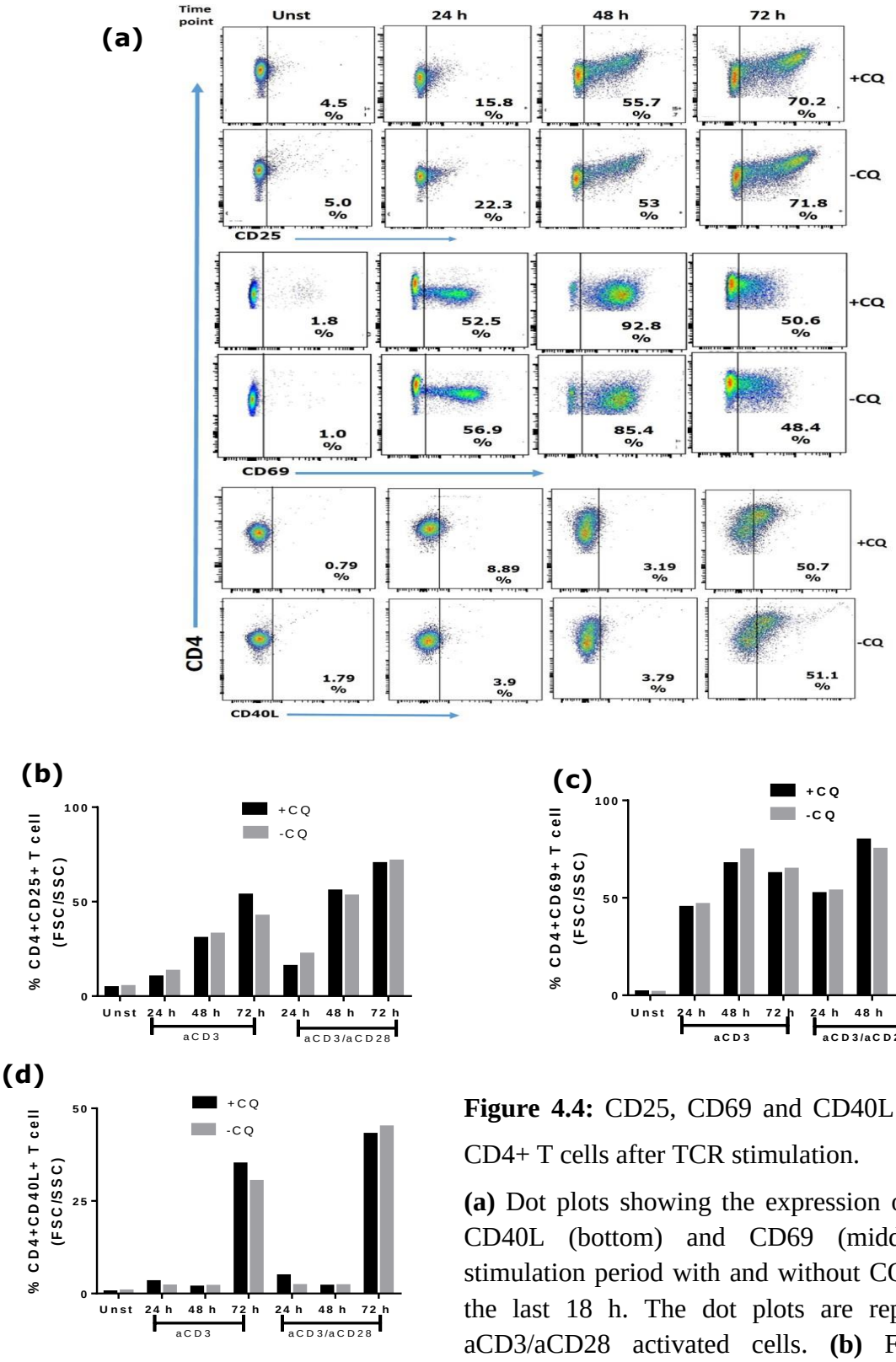

Figure 4.4: CD25, CD69 and CD40L expression on CD4+ T cells after TCR stimulation.

(a) Dot plots showing the expression of CD25 (top), CD40L (bottom) and CD69 (middle) over the stimulation period with and without CQ treatment for the last 18 h. The dot plots are representative of aCD3/aCD28 activated cells. **(b)** Frequencies of CD4+CD25+ expression over the stimulation period **(c)** Frequencies of CD4+CD69+ expression over the stimulation period **(d)** Frequencies of CD4+CD40L+ expression over the stimulation

period. Cells were stimulated with plate bound aCD3 alone and aCD3/aCD28 with and without CQ treatment for the last 18 h. Data is representative of two experiments showing similar outcome.

4.5 Combined analysis of autophagy and surface activation marker expression showed high levels of autophagy in activated CD4+ T cell subsets

We next attempted combined analysis of autophagy with CytoID and activation markers CD40L, CD25 and CD69 expression on CD4+ T cells. Regarding this, isolated CD4+ T cells were stimulated with plate bound aCD3 alone and aCD3/aCD28 in the presence or absence of CQ for the last 18 h, CytoID treated and phenotypically characterized as described in **3.3.1**, **3.3.3** and **3.2.2** respectively. Data was collected by flow-cytometry and gates were defined as in **Figure 4.1a** and the CD3+CD4+ T cell population was analyzed for the expression of CD40L, CD25 and CD69 (**Figure 4.5a**). Overlay of CytoID histogram plots normalized to mode were generated for the negative (red histogram) and positive (blue histogram) populations of CD40L, CD25 and CD69 expressing CD4+ T cells (**Figure 4.5b**). There was a moderate rightward histogram shift from CD4+ T cells without activation marker CD40L- or CD25- or CD69- to CD4+ T cells expressing activation marker CD40L+ or CD25+ or CD69+ respectively on the CytoID axis (**Figure 4.5b**).

Furthermore, CytoID MFI was quantified for CD4+ T cells with and without CD40L, CD69 and CD25 expression (**Figure 4.5c, d, e**). Activation marker expressing cells showed higher MFI (**Figure 4.5c, d, e**) for aCD3 alone and aCD3/aCD28 stimulated cells, which is suggestive of higher autophagy in activation marker expressing cells. The MFI level for activation marker expressing CD4+ T cells increased linearly over the stimulation period (**Figure 4.5c, d, e**). There seem to be no differences between the negative and positive populations of each activation marker at 24 h (**Figure 4.5c, d, e**). However, after 48 h increase in autophagy was observed in CD4+ T cells with high expression of activation markers (**Figure 4.5c, d, e**). Surprisingly, there were at the same time points no or only minimal differences in the level of autophagy observed in activation marker expressing CD4+ T cells stimulated with aCD3 alone or stimulated with aCD3/aCD28 (**Figure 4.5c, d, e**).

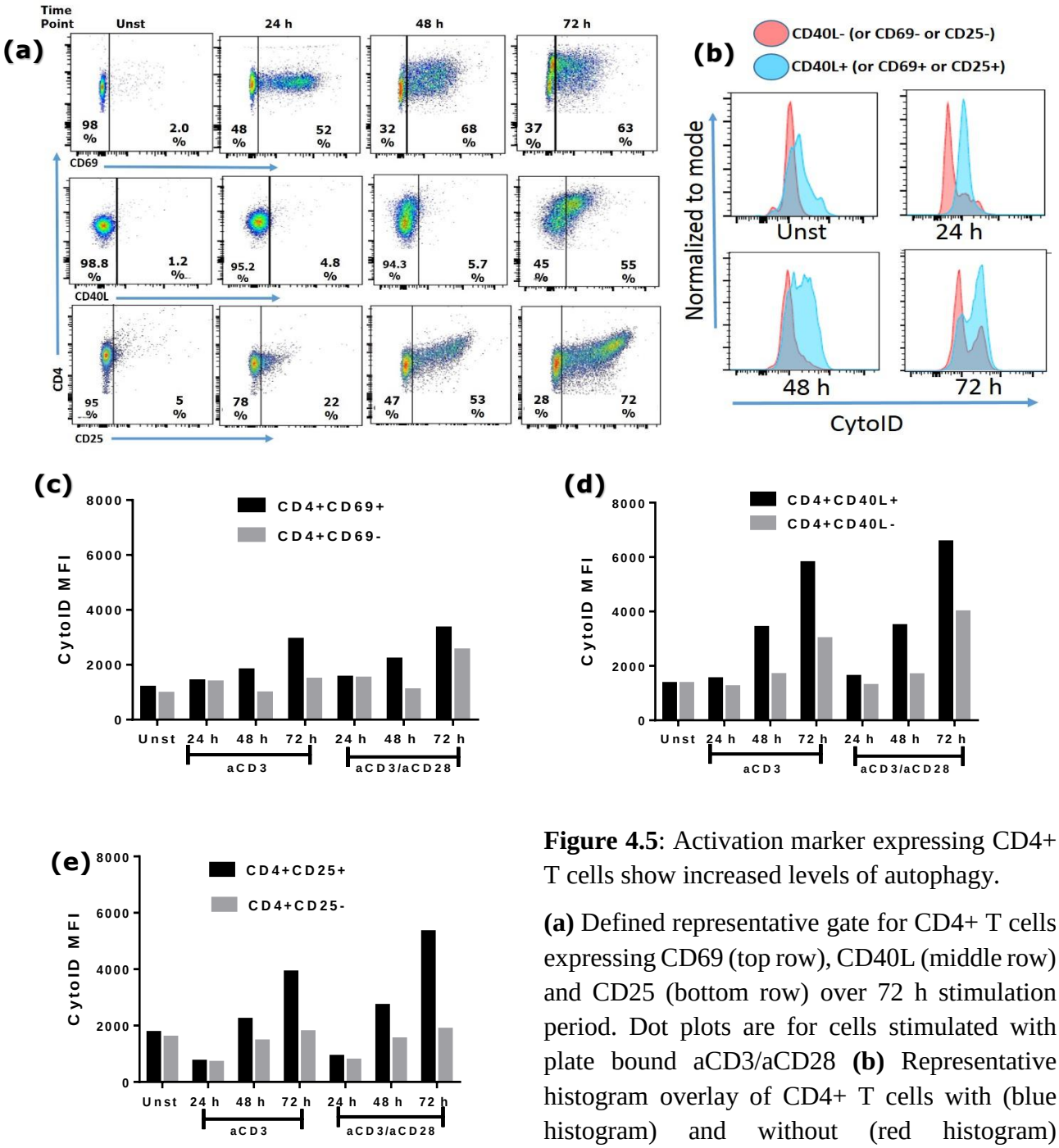

Figure 4.5: Activation marker expressing CD4+ T cells show increased levels of autophagy.

(a) Defined representative gate for CD4+ T cells expressing CD69 (top row), CD40L (middle row) and CD25 (bottom row) over 72 h stimulation period. Dot plots are for cells stimulated with plate bound aCD3/aCD28 **(b)** Representative histogram overlay of CD4+ T cells with (blue histogram) and without (red histogram) activation markers CD40L or CD25 or CD69 normalized to mode over the stimulation period. **(c, d, e)** Comparison of CytoID MFI for CD4+ T cells with and without activation markers CD69, CD40L and CD25 respectively. Each graph further compares MFI of CD4+ T cells with and without activation marker expression between aCD3 alone and aCD3/aCD28 stimulated cells over the 72 h period. The graphs in this panel were acquired from cells treated with CQ. This experiment was repeated twice with similar outcomes. aCD3 (8 µg/mL), aCD28 (2 µg/mL).

4.6 A large proportion of activated CD25+ T cells were found to produce effector cytokines and CD25+ T cells showed increased levels of autophagy

Activated CD4+ T cells can produce and secrete different types of effector cytokines which ultimately mediate CD4+ T cells effector functions. Unfortunately, we have found that measurement of autophagy using CytoID was not compatible with ICS in CD4+ T cells (**4.3**). Since, we have found that after TCR stimulation autophagy increased in activation marker expressing CD4+ T cells (**4.5**), we set-out to analyze to which extent CD25 and CD69 expressing CD4+ T cells produce IFN-γ, TNF-α and IL-2 effector cytokines. These CD4+ T cell effector cytokines are produced by CD4+ Th1 cells, which are known to be important in response to mycobacterial infections. A knowledge of the possibility that majority of the activated CD4+ T cells also produces effector cytokines would then, at least, allow us make an indirect correlation between effector cytokines (IFN-γ, TNF-α and IL-2) and autophagy. CD40L cannot make a good correlate due to its transient expression (**Figure 4.4d**) on stimulated CD4+ T cells.

To test if activation marker expression correlates with effector cytokine-production and autophagy, isolated CD4+ T cells were stimulated with plate bound aCD3 alone or aCD3/aCD28 for 24 h, 48 h and 72 h with or without CQ treatment for the last 18 h, as described previously (**4.1**). For the last 3 to 4 h of stimulation, protein transport inhibitor (PTI) was added. PTI blocks protein secretion pathways, thereby inducing ER stress and ER stress is also known to induce autophagy (106). Therefore, the effect of PTI on autophagy induction was assessed over a 5 h period. PTI did not induce autophagy in activated CD4+ T cells after 5 h of PTI treatment (**Appendix V**) and thus should not interfere with analysis of autophagy induced after TCR stimulation.

In order to make this correlation, stimulated cells were treated for analysis in two subsets. Thus combined activation marker staining with ICS for effector Th1 cytokines and combined activation marker staining with CytoID staining without ICS. For combined activation marker and ICS, the stimulated CD4+ T cells were harvested, stained with fixable viability dye and antibodies against surface activation markers CD25 and CD69, before fixation and permeabilization for ICS (as outlined in **3.2.2**). In parallel, aliquots of the identically stimulated cells were stained with CytoID, fixable viability dye and antibodies against surface activation markers CD25 and CD69 but without

fixation and permeabilization for ICS. Cells treated with CytoID dye were used in autophagy analysis in CD25 and CD69 expressing CD4+ T cells. In contrast, those without CytoID treatment were used for IFN-γ, IL-2 and TNF-α analysis in CD25 and CD69 expressing CD4+ T cells. Data was collected and gates were defined for CD3+CD4+ T cell population as described previously (**Figure 4.1a**).

Activation marker gates for CD25 and CD69 negative, single and double positive CD4+ T (CD25-CD69+, CD25+CD69+, CD25+CD69- and CD25-CD69-) cells were then defined for all samples from the CD3+CD4+ T cell population (**Figure 4.6a**). For the samples where ICS for effector Th1 cytokines but not CytoID staining was performed, gates for IL-2, TNF-α and IFN-γ were defined from unstimulated negative control cells and applied for CD25-CD69+, CD25+CD69+, CD25+CD69- and CD25-CD69- gated CD4+ T cells (**Figure 4.6a, TNF-α not shown**). The observed frequencies of TNF-α producing CD4+ T cells were very low (Data not shown). Next, the frequencies of the sum of IFN-γ and IL-2 was compared for CD25-CD69+, CD25+CD69+, CD25+CD69- and CD25-CD69- gated CD4+ T cells over the stimulation period for aCD3 alone and aCD3/aCD28 stimulated cells (**Figure 4.6b**). Comparatively, more cytokine (IFN-γ and IL-2) production was observed in aCD3/aCD28 than aCD3 activated cells over the stimulation period. At 24 h maximum total cytokine production (IFN-γ and IL-2) was observed (40-70 % for aCD3/aCD28 vs 25-60 % for aCD3 alone) for CD25+CD69+, CD25+CD69-, CD25-CD69- and CD25-CD69+ gated CD4+ T cells and this slowly decreased at later time-points (**Figure 4.6b**). CD4+ T cells expressing CD25 as well as CD69 (CD25+CD69+ cells) showed high proportion of IL-2 and IFN-γ production over the stimulation period. This was followed by the CD25+CD69- and CD25-CD69+ cell population. The CD25-CD69- cell population not expressing any of the activation markers showed the lowest proportion of IFN-γ and IL-2 production, although cytokine-producing T cells were also found in this population, especially at the 24 h time-point (**Figure 4.6b**).

In parallel to the combined activation marker and ICS for effector Th1 cytokines, identically activated samples (aliquots from each sample used for activation marker and ICS analysis) were stained for surface activation marker CD25 and CD69 expression in combination with CytoID staining to assess autophagy. These latter samples were not stained for intracellular effector Th1 cytokines which allowed us to obtain information on autophagy-induction in different subsets of

CD25 and CD69 negative, single and double positive CD4+ T cells after TCR stimulation. Data was analyzed and CytoID MFI was quantified from the histogram plots (**Appendix VI**) generated from CD25+CD69-, CD25+CD69+, CD25-CD69+ and CD25-CD69- gated CD4+ T cells at each time point over the stimulation period and the quantification is summarized in **Figure 4.6c**. At 24 h post activation, the MFI in all subsets were found comparable to the MFI of unstimulated samples indicating no induction of autophagy in the samples after 24 h. However, after 48 h and even more at 72h, autophagy was induced as measured by increased CytoID MFI. At 48 h, MFI of CytoID was found in CD25+CD69+ and CD25+CD69- cells to be an 0.5-fold more than the MFI of CD25-CD69+ and CD25-CD69- cell population. This was even found to more after 72 h with an 2.5-fold increase in MFI for CD25+CD69+ and CD25+CD69- cells compared to CD25-CD69+ and CD25-CD69- cell population. CytoID MFI in CD25-CD69+ and CD25-CD69- cells at 48 and 72 h (about 1900 MFI) were observed to be at the level of unstimulated samples (**Figure 4.6c**). This suggest that CD25+T cells are those that upregulate autophagy 48 and 72 h after TCR stimulation in CD4+ T cells. This was independent of CD69 expression, as CD69 expression alone did not correlate with autophagy. Correlation of CD25 with autophagy is very interesting since both CD25 expression and autophagy follow similar kinetics of upregulation between 48 and 72h (**Figure 4.6a, c**).

The combined CytoID and surface activation marker staining showed that CD25+ cells (CD25+CD69+ and CD25+CD69-) are the main CD4+ T cells that induce and upregulate autophagy, as CD69 expression does not correlate with autophagy (**Figure 4.6c).** Furthermore, from combined surface activation marker and ICS for effector Th1 cytokines (**Figure 4.6b**), we found high levels of IL-2 and IFN-γ effector cytokine production in all cell subsets at 24 h. But at 48 and 72h (when autophagy was induced), we observed that it was the CD25+ subsets of CD4+ T cells that produce most of the cytokines (IFN-γ and IL-2) (CD25+CD69+ showed higher frequency than CD25+CD69-). Therefore, taking **Figure 4.6b** and **c** together, CD69 (an early activation marker) is not a good correlate for cytokine production and autophagy induction at 48 and 72 h after TCR stimulation. However, at 48 and 72 h most of the IFN-γ and IL-2 producing CD4+ T cells were found in the CD25+ population and they were also the same subset that induced and upregulated autophagy. In sum, analysis of autophagy in CD25+T cells could be a possible correlate to estimate autophagy in effector Th1 cytokine-producing cell population.

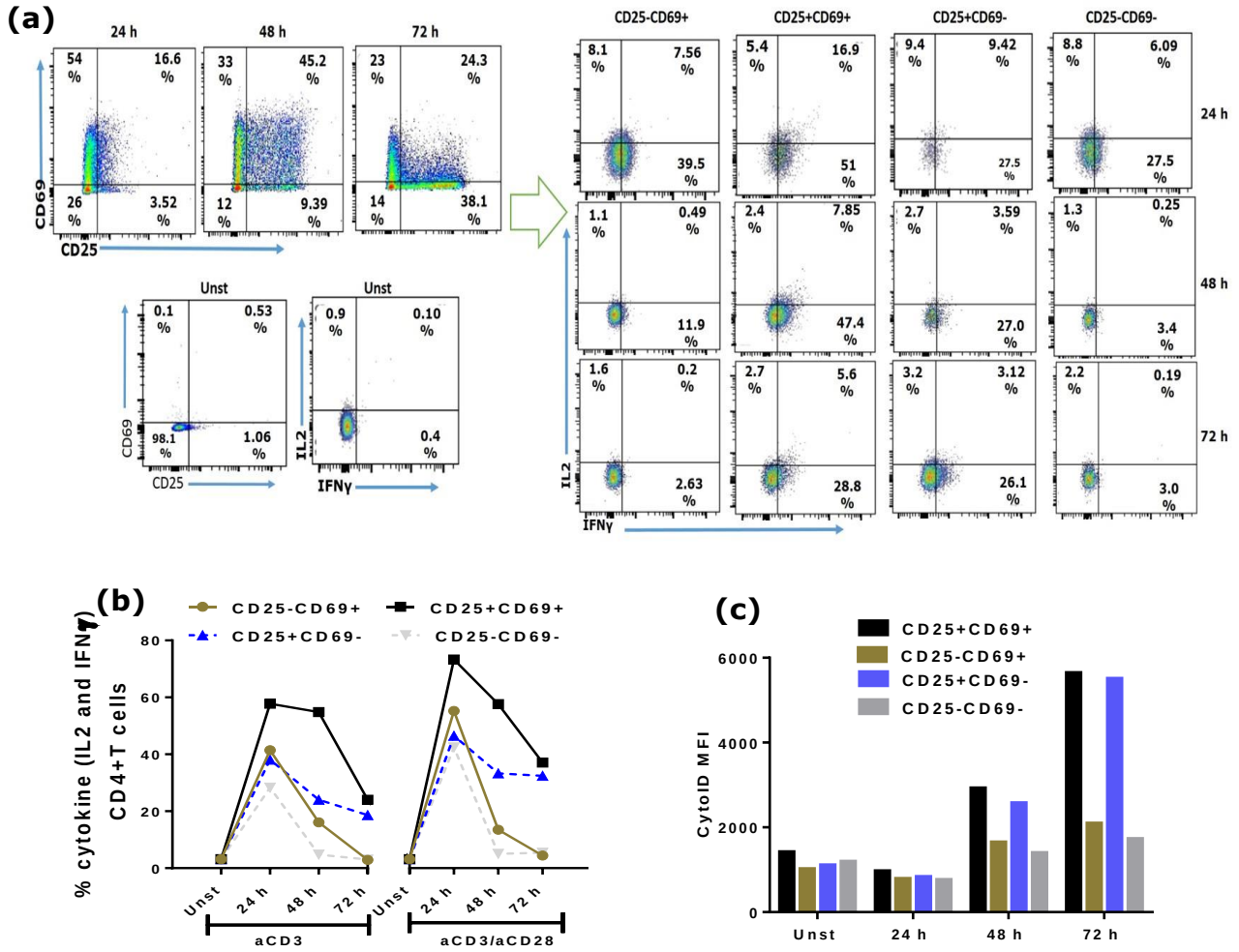

Figure 4.6: Effector-cytokine production (IFN-γ and IL-2) and autophagy in different subsets of activated CD4+ T cells.

(a) Example of the gating strategy to identify activation marker gates for CD25 and CD69 negative, single or double positive CD4+ T (CD25-CD69+, CD25+CD69+, CD25+CD69- and CD25-CD69-) cells, as well as the frequency of IFN-γ and IL-2 in the different activation marker subsets (CD25-CD69+, CD25+CD69+, CD25+CD69- and CD25-CD69-). The dot plots shown are representative of cells stimulated with aCD3/aCD28 over the stimulation period. Stimulated CD4+ T cell samples used in this gating were extracellularly stained for CD25 and CD69 before fixation and permeabilization for effector Th1 ICS **(b)** The sum of the frequencies of IFN-γ and IL-2 produced in the CD69 and CD25 negative, single or double positive CD4+ T cell population over the stimulation period. The cytokine profile is a comparison of aCD3 alone and aCD3/aCD28 stimulated CD4+ T cells over the stimulation period. This data was from cell samples which were surface stained for activation markers before fixation and permeabilization for ICS. Cells used for effector Th1 cytokine analysis were not CQ treated **(c)** Autophagy measured by quantification of CytoID MFI from CD25-CD69+, CD25+CD69+, CD25+CD69- and CD25-CD69- gated CD4+ T cells over the stimulation period. Results shown are from cells stimulated with plate bound

aCD3/aCD28 for 24 h, 48 h, and 72 h as well as unstimulated samples, which were CytoID stained along with extracellular CD25 and CD69 staining without fixation and permeabilization for ICS. Cells used in autophagy quantification were treated with CQ for the last 18 h of culture. This experiments were performed once. aCD3 (8 µg/mL), aCD28 (2 µg/mL).

4.7 Combined analysis of autophagy and effector-cytokine production using a method avoiding cell permeabilzation reveals upregulated autophagy in IFN-γ-producing CD4+ T cells

Previous results (**4.6**) have shown that analysis of autophagy in CD25+ (but not CD69+) activated T cells may represent a possible correlate to study autophagy in the population of cytokine-producing (IFN-γ and IL-2) CD4+ T cells. However, not all CD25+ T cells were found to produce effector Th1 cytokines (**Figure 4.6b**) and the expression of CD25 on CD4+ T cells may not predict which cytokines would be produced. In addition, combination of CytoID with ICS was found to be problematic (**4.3**). Therefore, we attempted combined analysis of surface activation marker, autophagy and direct effector cytokine staining utilizing a fluorescent tagged IFN-γ catch reagent. For this purpose, secreted IFN-γ effector cytokine from CD4+ T cells were analyzed with the aid of the IFN-γ catch reagent (as described in **3.3.2**) in combination with surface activation marker staining and autophagy analysis with CytoID. The cytokine catch reagent does not require fixation and permeabilization procedures to detect IFN-γ production from CD4+ T cells.

Isolated CD4+ T cells were stimulated 48 h with plate bound aCD3/aCD28, in the presence and absence of CQ for the last 18 h. The cells were harvested and then subjected to the IFN-γ secretion assay protocol (**3.3.2**). In short, stimulated cells were labelled with IFN-γ catch reagent and incubated for a secretion period for 45 min at 37 ^{0}C during which secreted IFN-γ binds to the IFN-γ-catch-reagent attached to the surface of the intact cell. Subsequently, the cells were incubated with a fluorescent IFN-γ detection antibody, stained with CytoID dye (**3.3.3**) and then extracellularly phenotyped (**3.2.2**). Using this method, we were able to analyze autophagy with the CytoID dye in addition to CD25 activation marker and IFN-γ staining as cells were not fixed and permeabilized. Gates were defined for CD3+CD4+ T cells as shown in **Figure 4.1a**. From the

CD3+CD4+ gated T cell population, CD25+ and CD25- gates were defined (**Figure 4.7a**). Furthermore, from the CD25+ and CD25- gates, IFN-γ gates were then defined (**Figure 4.7a**). Overlay of CytoID histogram plots were then generated for CD25-positive (CD25+IFN-γ+ and CD25+IFN-γ- cells) and CD25-negative (CD25-IFN-γ+ and CD25-IFN-γ-) CD4+ T cell subsets (**Figure 4.7a**). MFI of CytoID was then quantified from each histogram overlay (**Figure 4.7b**). CD25+IFN-γ+ expressing CD4+ T cells showed the highest level (4500 MFI) of autophagy, followed by CD25+IFN-γ- cells (3500 MFI) and then CD25-IFN-γ+ (1800 MFI), whereas unactivated non-cytokine producing CD25-IFN-γ- showed basal levels of autophagy which were comparable to autophagy in negative control (1500 MFI) samples (**Figure 4.7b**). Taking together, these results demonstrate that autophagy can be quantified in specific cytokine-producing cell using the cytokine secretion assay method to identify effector-cytokine producing CD4+ T cells. Thus, the use of this method overcomes the problem of quantifying autophagy in cytokine producing CD4+ T cells that were initially observed when attempting to combine CytoID staining with ICS.

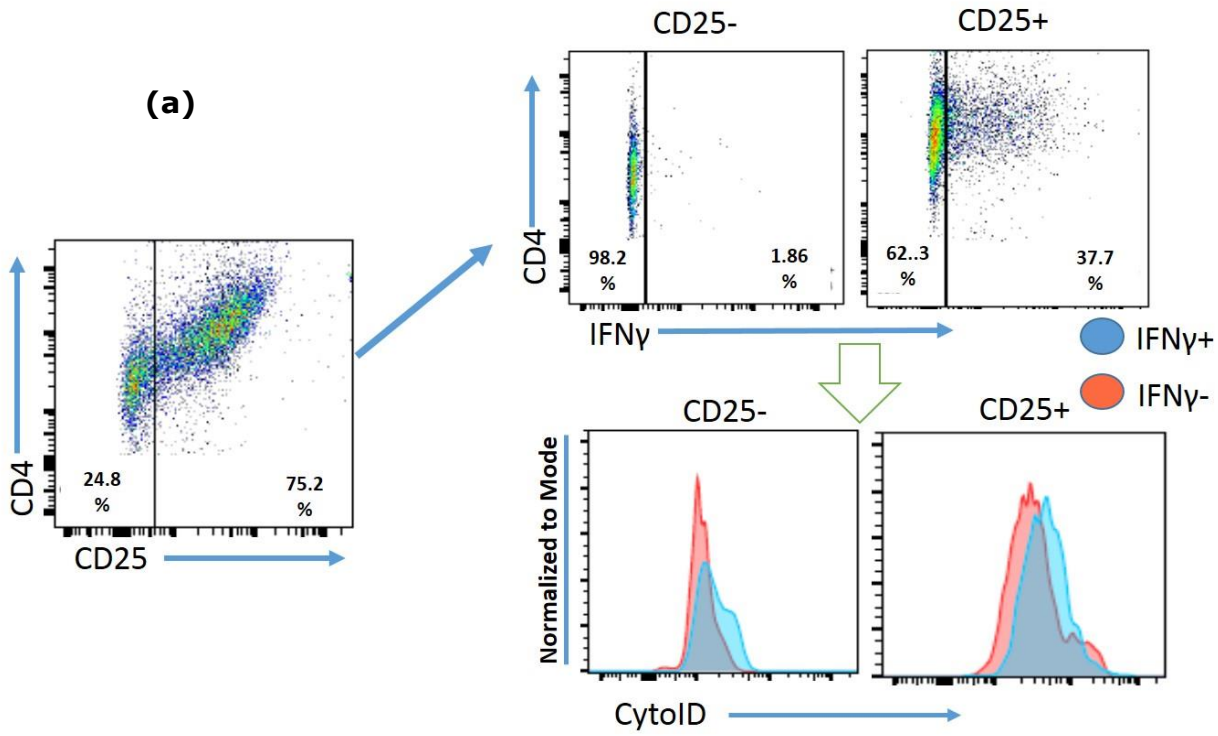

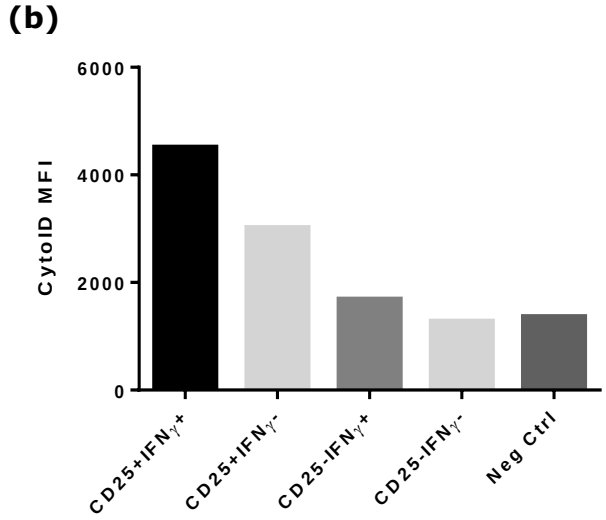

Figure 4.7: Direct analysis of autophagy in IFN-γ specific CD4+CD25+T cells using a cytokine secretion assay.

(a) Example of gating strategies for CD4+ T cells with and without CD25 expression after 48 h of stimulation. From the CD25+ and CD25- population, IFN-γ+ and IFN-γ- gates were defined, and overlays of CytoID histogram plots were generated for CD25+IFN-γ+ and CD25+IFN-γ- cells, and CD25-IFN-γ+ and CD25-IFN-γ- cells**. (b)** Quantified CytoID MFI for CD25+IFN-γ+, CD25+IFN-γ-, CD25-IFN-γ+ and CD25-IFN-γ- cells. Cells were stimulated with plate bound aCD3/aCD28 for 48 h and data are for CD4+ T cells without CQ treatment. This experiment was repeated twice with similar outcomes. aCD3 (8 µg/mL), aCD28 (2 µg/mL).

4.8 Hypoxia upregulates TCR stimulation-induced autophagy and cytokine production

Previous results have shown that autophagy could directly be quantified in effector cytokine specific (IFN-γ) CD4+ T cells using the cytokine secretion assay (**4.7**). We then proceeded to quantify autophagy in IFN-γ-producing CD4+ T cells stimulated under hypoxic conditions. For this purpose, isolated CD4+ T cells were stimulated with plate bound aCD3/aCD28 for 48 h under hypoxic (2 % O_2) and normoxic (ca. 20% O_2) conditions. For the last 18 h of stimulation, CQ was added and, autophagy and IFN-γ production were analyzed with CytoID dye and the IFN-γ secretion assay (as in **4.7**) respectively. CD3+CD4+ T cells were identified as previously described (**4.1a**) and overlays of CytoID histogram plots were generated for CD4+ T cells (**Figure 4.8a**). There was no difference in the histogram plots for unstimulated cells under normoxic and hypoxic conditions, indicating that hypoxia do not affect the levels of basal autophagy in unstimulated cells (**Figure 4.8a**). In contrast, we found increased levels of autophagy (as measured by increased CytoID MFI) in CD4+ T cells cultivated under hypoxia compared to CD4+ T cells cultured under normoxic conditions after 48 h of stimulation. From the overlay of histogram plots, CytoID MFI were quantified for cells stimulated under normoxic and hypoxic conditions (**Figure 4.8c)**. CytoID MFI in total CD3+CD4+ T cells was almost doubled (1.9-fold increased) under hypoxia compared to cells culture normoxic conditions. Further, IFN-γ+ and CD25+ gates were also defined from the CD3+CD4+ gated T cell population (**Figure 4.8a**). We saw an increase in CD4+ T cells expressing CD25+ and IFN-γ+ under hypoxic condition compared to normoxic conditions (**Figure 4.8a, b**). The frequencies of CD25+ and IFN-γ+ T cells both showed an 1.6-fold increase under hypoxic conditions compared to normoxic conditions. These findings suggest that CD4+ T cells show higher levels of activation, cytokine-production and autophagy under hypoxic conditions (**Figure 4.8b**). From the CD25+ and CD25- gate (as in **Figure 4.8a**), IFN-γ gates were defined for CD4+ T cells cultured under normoxic and hypoxic conditions. We observed that for CD4+CD25+T cell population, more IFN-γ+ was produced under hypoxia compared CD4+ T cells cultured under normoxic conditions (**Figure 4.8d**). However, for CD4+CD25-T cell population there was no difference in the level of IFN-γ production for normoxia and hypoxia cultured CD4+ T cells (**Figure 4.8d**). Furthermore, CytoID overlay of histogram plots were generated for the CD25-positive (CD25+IFN-γ+ and CD25+IFN-γ-) and CD25-negative (CD25-IFN-γ+ and CD25-IFN-

γ-) CD4+ T cell population cultured under hypoxic and normoxic conditions (**Figure 4.8d**). CytoID MFI was then generated from the histogram overlays (**Figure 4.8e**). We observed increased MFI in CD25+IFN-γ+ (2500-3000 MFI) cell population compared to CD25+IFN-γ- (1500-2000 MFI) cell population cultured under normoxic and hypoxic conditions. MFI observed for CD25-IFN-γ- and CD25-IFN-γ+ cells were at the level of the negative unstimulated (1000-1100 MFI) control (**Figure 4.8e**). In addition, relatively more autophagy (as measured by MFI) was observed in CD25+IFN-γ+ and CD25+IFN-γ- cell population for CD4+ T cells cultured under hypoxia compared to their normoxia counterparts (**Figure 4.8e**). Taking together, **Figure 4.8d** and **e** suggests that regardless of IFN-γ production, hypoxia upregulate autophagy in CD4+CD25+T cells and IFN-γ production may influence autophagy levels in CD25+ cells as differences were observed in autophagy (measured by CytoID MFI) levels between IFN-γ- and IFN-γ+ population of CD25+ cells.

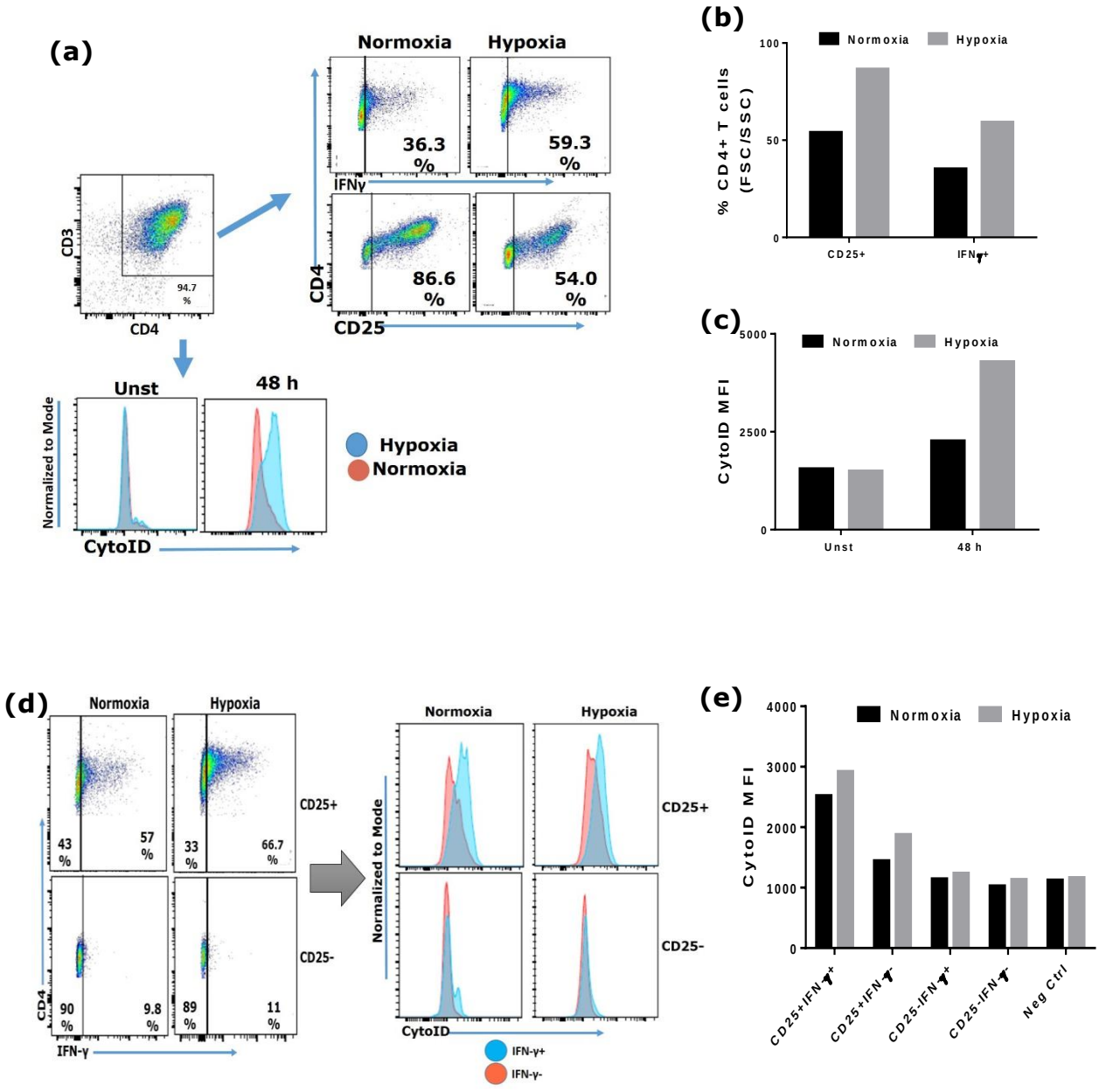

Figure 4.8: Hypoxia upregulates autophagy, activation marker expression and IFN-γ levels in activated CD4+ T cells.

(a) Dot plots showing IFN-γ and CD25 expression from the CD3+CD4+ gated T cells analyzed by surface activation marker staining and cytokine secretion assay as described in **4.7**. Further, from the CD3+CD4+ gated T cells an overlay of CytoID histogram plots were generated for CD4+ T cells stimulated under normoxic and hypoxic conditions 48 h post stimulation with aCD3/aCD28. **(b)** Frequencies of CD25+ and IFN-γ+ expressing CD4+ T cells under normoxic and hypoxic conditions as defined by gates in **a**. **(c)** Quantified CytoID MFI from the overlays of CytoID histogram plots under normoxic and hypoxic condition in **a**. (**d**) Dot plots showing IFN-γ gates on the CD25+ and CD25- populations defined in **a**, for cells stimulated under hypoxic and

normoxic condition after 48 h. From the IFN-γ+ and IFN-γ- cell population, overlays of histogram plots were generated for the CD25-positive (CD25+ IFN-γ+ and CD25+ IFN-γ-) and CD25-negative (CD25-IFN-γ+ and CD25-IFN-γ-) cell population for normoxia and hypoxia cultured cells. (**e**) CytoID MFI for CD25+ IFN-γ+, CD25+ IFN-γ-, CD25- IFN-γ+ and CD25- IFN-γ- cell population stimulated under hypoxic and normoxic conditions for 48 h. This experiment was performed once and data was for CD4+ T cells stimulated without CQ treatment.

4.9 Preliminary results indicate that mycobacteria-specific CD4+ T cells can be expanded from healthy donors

Using CytoID in combination with cytokine secretion assay, we were able to directly analyze autophagy in effector-cytokine producing CD4+ T cells under different conditions such as hypoxia and normoxia. However, all experiments so far were performed with polyclonally activated CD4+ T cells using aCD3/aCD28. Mycobacteria-specific CD4+ T cells can be found in healthy donors but they occur at relatively low frequencies (107). These antigen-specific T cells can be selectively expanded *in vitro* with antigen presented from autologous APCs to increase the frequencies of the specific T cells through proliferation and differentiation.

Isolated CD4+ T cells were expanded with heat killed *M. avium* presented from autologous antigen-presenting cells for 13 days as described in **3.1.5** to generate mycobacteria-specific CD4+ T cells. Two different types of media (TexMACS and RPMI-complete media) were compared to optimize expansion protocols for mycobacteria-specific CD4+ T cells. In parallel, autologous MDMs were generated (**3.1.6**) from the same donor. On day 13, expanded T cells were re-stimulated with autologous MDMs that were pre-incubated overnight with mycobacterial antigens as described in **3.1.7**. Expanded antigen-specific T cells were re-stimulated for 24 h with PTI present for the last 4 h of culture. The cells were then harvested and phenotyped as described in **3.2.2**. Gates were defined for CD3+CD4+ T cells as described previously in **Figure 4.1a**. From the CD3+CD4+ gated T cells, IFN-γ, IL-2 and TNF-α gates were defined, which are known effector cytokines produced by mycobacteria-specific CD4+Th1 cells (**Figure 4.9a**). Up to 20 % of CD4+ T cells were found to produce IFN-γ after re-stimulation with heat killed *M. avium* (**Figure 4.9b, c**). The dose of mycobacterial antigen had minimal effect with respect to the cytokine levels of mycobacteria-specific CD4+ T cells. Thus, the use of heat killed *M. avium* at a MOI of 1

and 10, both yielded about 25 % of IFN-γ, 12 % of IL-2 and 10 % of TNF-α. The level of IL-2 and TNF-α production was observed to be 2 to 2.5-folds lower than IFN-γ production after re-stimulation (**Figure 4.9b, c**). Furthermore, TexMACS media expanded CD4+ T cells yielded 28 % IFN-γ, 13 % IL-2 and 11 % TNF-α. In contrast, RPMI-complete media yielded 20 % IFN-γ, 5 % IL-2 and 5 % TNF-α. In addition, TexMACS media expanded cells showed high background (6 to 8 %) compared to RPMI-complete (2 to 4 %) media with respect to IFN-γ, IL-2 and TNF-α levels in unstimulated cells. TexMACS media seems more suitable to expand mycobacteria-specific CD4+ T cells and to enable the expanded T cells to produce more IFN-γ effector cytokine upon re-stimulation (**Figure 4.9b, c**). Expansion protocol seems to work, however, significant frequency of IFN-γ-producing CD4+ T cells was not expanded from all donors. The expansion protocol requires optimization to enable stable expansion of *Mycobacterium*-specific CD4+ T cells. In order to enable the study of autophagy and cytokine production in mycobacteria-specific CD4+ T cells under hypoxic conditions as seen in granuloma of TB patients.

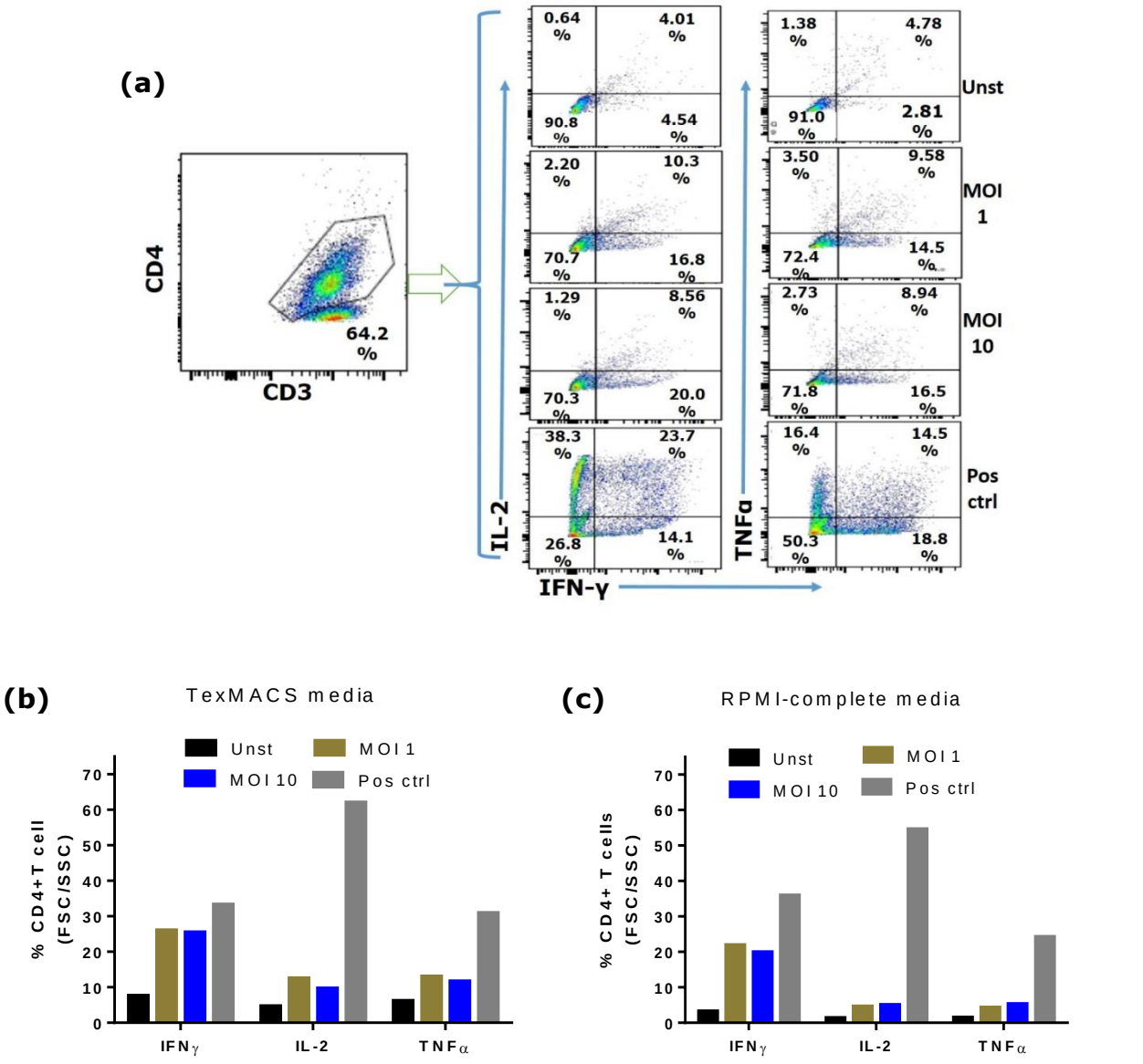

Figure 4.9: Expansion of primary human mycobacteria-specific CD4+ T cells from a healthy donor.

(**a**) CD4+ T cells from healthy donors expanded for 13 days in RPMI-complete media and TexMACS media. The expanded cells were re-stimulated with autologous macrophages, which were pre-stimulated with heat killed *M. avium* overnight. After re-stimulation, the cells were treated 4 h with PTI before phenotyping intracellularly for IFN-γ, IL-2 and TNF-α and extracellularly with anti-CD3 and -CD4 antibodies for flow-cytometry. Gates were defined on the CD3+CD4+ T cell population as in **4.1a** and from the CD3+CD4+ gated T cell population, IFN-γ (X-axis) and, IL-2 and TNF-α (Y-axis) gates were defined. Dot plots are representative of CD4+

T cells expanded in TexMACS media (**b**) Analyzed frequencies of IL-2, TNF-α and IFN-γ produced by mycobacteria-specific CD4+ T cells expanded in TexMACS media (**c**) Analyzed frequencies of IL-2, TNF-α and IFN-γ produced by mycobacteria-specific CD4+ T cells expanded in RPMI-complete media. Expansion of mycobacteria-specific CD4+ T cells was successfully performed from two healthy donors with similar outcomes.

5 Discussion

The growing significance attached to autophagy in development and disease in eukaryotes has informed the need to validate reliable, meaningful and quantitative methods that appropriately and accurately measure autophagy in cells (105). The aim of this study was to develop assays and utilize them to study autophagy in different subsets of mycobacteria-specific CD4+ T cells under hypoxic conditions. In this regard, we have shown that autophagy can reliably be quantified in primary human CD4+ T cells by a flow-cytometric method using a novel fluorescent probe CytoID green detection dye. We have also shown that this method allows direct analysis of autophagy in different subsets of primary human CD4+ T cells after activation. Unfortunately, CytoID green detection dye could not be combined with intracellular CD4+ T cell effector cytokine staining on the same cells. Due to the lack of this possibility, we demonstrated that autophagy in activation marker CD25 expressing CD4+ T cells could indirectly, to some extent be correlated to effector cytokine (IFN-γ and IL-2) levels in CD25 expressing CD4+ T cells. Finally, we were able to establish a novel way of directly quantifying autophagy in specific effector cytokine (IFN-γ), producing CD4+ T cells with a technique independent of intracellular cytokine staining. Interestingly, preliminary experiments with this method have shown that hypoxia upregulates TCR stimulation-induced autophagy and IFN-γ production. To now study autophagy in antigen-specific CD4+T cells, we have developed an assay to expand primary human mycobacteria-specific CD4+ T cells from healthy donors. Even though not fully optimized, this might allow onward direct studies of autophagy in mycobacteria-specific effector CD4+ T cells under hypoxic conditions.

The hallmark of an immune response to mycobacteria infection is the formation of granuloma. The granuloma environment is said to be characterized by hypoxia (~0.2 % O_2) (52, 55, 59, 85, 108). Hypoxia induces the stabilization of HIF-1α, a transcription factor that is believed to be a central regulator of cellular survival in response to hypoxia (61). In peripheral T cells, HIF-1α signaling was shown to suppress activation-induced T cell death mediated by TCR stimulation (88). Thus, HIF-1α signaling enhances the survival of peripheral T cells. Furthermore, Th1 cells at the site of persistent phagosomal infections that result in granuloma formation acquire the ability to produce anti-inflammatory cytokine IL-10 (89). In addition, signaling through IL-10 receptor suppresses the IFN-γ and TNF-α production in CD4+ T cells (90, 91). Also, IFN-γ production by antigen-specific CD4+ T cells in granuloma-associated infections was shown to deteriorate progressively

over time (89). Early production of IL-10 during CD4+ T cell priming phase negatively affected antigen-specific CD4+ T cell expansion, maintenance and function in this study. Further, it is also known that IL-10 signaling inhibits autophagy (83, 92). In sum, these studies raise the question of how autophagy will be regulated in granuloma associated antigen (mycobacteria)-specific-CD4+ T cells, and does this influence CD4+ T cell effector cytokine-production? Furthermore, specific CD4+ effector T cell response to infection can be characterized by the cytokine profile produced in response to stimulation with antigen. Autophagy is induced upon T cell activation and autophagy is necessary for cytokine production (22), proliferation, survival, memory formation and differentiation (93) of T cells. To our knowledge, there are no methods available which measures autophagy along with effector cytokines in primary human antigen-specific T cells.

Currently, the ‘‘gold standard’’ for monitoring autophagy has been LC3II quantification by immunoblotting, together with electron microscopy for autophagosome formation as well as confocal microscopy. LC3II is the lipidated form of LC3I. During the induction of autophagy LC3I is converted to LC3II, which is incorporated into the growing autophagosome. Hence, LC3II quantification is a good marker for autophagy. However, concerns are that LC3 expression might differ in response to various stress stimuli and between different cell types. Also, overexpression of fluorescent tagged-LC3 can be used to facilitate visualization of autophagy by imaging techniques interfere with autophagy in itself (105).

In this study, autophagy was quantified by a novel flow-cytometric method using CytoID dye. CytoID is a cationic amphiphilic fluorescent probe, which according to the manufacturer specifically stains autophagosomes and autophagolysosomes. This dye, even though scanty information is provided by the manufacturer about the dye, presents the opportunity to study autophagy in live cells with the help of a flow-cytometer without the need for transfection. Flow-cytometry measures and analyzes multiple physical parameters of single cells. The properties measured include particles size, internal complexity and relative fluorescence intensity. Measuring CytoID fluorescence intensity would suggest the proportion or number of autophagosomes formed, since the dye specifically stains autophagosomes, which could also be referred to as autophagsosome abundance. The flow-cytometric method was used to study autophagy in activated primary human CD4+ T cells and the observed outcome corresponds to LC3II immunoblotting, which confirms the validity of CytoID to study autophagy.

TCR stimulation has been shown to induce autophagy and the induction of autophagy is necessary to support CD4+ T cells activation (22). This effect may, at least in part, be due to the metabolic needs for proliferation, differentiation and the synthesis of effector molecules after activation. We have shown here that autophagy is induced in CD4+ T cells using various TCR stimulation reagents by flow-cytometry using CytoID dye as well as LC3II immunoblotting. Autophagy results in release of the degraded macromolecules into the cytosol for reuse in ATP synthesis to maintain the viability of cells under conditions of stress (109). This suggests that the increasing autophagosomes (autophagy) observed over the TCR stimulation period may be geared towards ATP synthesis. This further implies that the extent to which CD4+ T cells are activated may be proportional to the energy-need of the cells.

T cell activation involves signaling through TCR and CD28 (42). Anti-CD3/aCD28 mimics physiological T cell activation and as such our results showed highest levels of autophagy in CD4+ T cells stimulated with plate bound aCD3/aCD28, although our results suggest that TCR stimulation without costimulatory aCD28 signal is enough to induce autophagy in primary human CD4+ T cells. This effect may be due to the fact that TCR stimulation via signal one (by plate bound aCD3 alone) mediates signaling processes which leads to CD4+ T cell activation.

As a consequence of TCR signaling, CD40L and CD69 mRNA synthesis is mediated by NFAT signaling via the phosphatase calcineurin. This is because, calcineurin pathway inhibitor cyclosporine A has been shown to greatly inhibits CD40L and CD69 expression (47, 110, 111). Our results showed no clear differences in CD69 and CD40L expression between aCD3 and aCD3/aCD28 activated CD4+ T cells since calcinerin signaling is mediated mainly by signal one (via TCR stimulation without co-stimulation) after TCR stimulation. The efficient expression of lymphokine (IL-2 and IFN-γ) and lymphokine receptor [e.g., IL-2R (CD25) and IFNR] genes appears to require signaling through TCR and CD28. Signaling through CD28 has been associated with the mRNA stabilization of lymphokine and lymphokine receptor genes and increased IL-2 promotor activity (112, 113). Our data suggest higher expression of CD25, IFN-γ and IL-2 in aCD3/aCD28 compared to aCD3 activated cells, which may be due to the stabilization effect of CD28 signaling on lymphokine and lymphokine receptor mRNA. This effect may partly be responsible for the high expression of IFN-γ and IL-2 in CD25+ cells, since efficient CD25, IFN-γ and IL-2 expression are tied to lymphokine mRNA stabilization.

CD4+ T cells produce and respond to IL-2. IL-2 signaling occurs through the IL-2R (also known as CD25) and it is known to induce the cells to enter the cells cycle for differentiation and proliferation (114). However, IL-2R is expressed upon TCR stimulation (115). Our results showed that CD25+ (CD25+CD69+ and CD25+CD69-) but not CD69+ (CD25-CD69+) expressing CD4+ T cells induced and upregulated autophagy, probably due to the induction of extensive proliferation and differentiation by IL-2 in CD25 expressing cells. Therefore, autophagy was appropriately upregulated to sustain the energy demand for proliferation and differentiation. Anti-CD28 on the other hand induces signaling through the costimulatory molecule CD28 and is required for full T cell activation. Signaling through CD28 requires TCR stimulation for T cell activation (42, 116) but CD28 alone may not induce activation in T cells. We exploited anti-CD28 and IL-2 without prior TCR stimulation with aCD3 for their ability to induce autophagy. Results showed only basal level of autophagy at all time-points, suggesting that IL-2 and anti-CD28 alone are unable to induce activation and autophagy in CD4+ T cells.

Autophagy flux analysis is a necessary requirement to appropriately study autophagy regulation in eukaryotic cells (105). In this study, two chemical inhibitors of autophagy BAF A1 and CQ were used for autophagy flux analysis. In the presence of these inhibitors, the accumulation of autophagosomes would be evident of efficient autophagy flux, while failure of autophagosome accumulation in the presence of BAF A1 and CQ, would predict a defect or delay in the earlier processes along the autophagy pathway, prior to degradation at the autophagolysosome. BAF A1 and chloroquine are Na+H+ pump and vacuolar ATPase inhibitors respectively. They are known to partially inhibit the degradation of autophagolysosome content by increasing lysosomal pH thereby inhibiting acidic lysosomal protease activity (105, 117, 118). Our data have shown increased autophagosome abundance in the presence of both BAF A1 and CQ, which suggest an efficient autophagy flux. This was expected and further confirms that autophagy was actually measured by our method. In addition, inhibition of autophagy flux by CQ did not affect the expression of activation markers CD40L, CD25, and CD69, which suggests that the synthesis of activation marker might not be an energetically demanding cellular process. Furthermore, CD40L expression on activated CD4+ T cells is transient. After TCR stimulation, CD40L mRNA peaks at 1-4 h, and the surface expression of its protein is around 4-6 h. This is rapidly shed after 16-18 h (110). Our results showed minimal expression of CD40L at 24 and 48 h, indicating that at these time points CD40L may have been shed. However, at 72 h there were high levels of CD40L

detected. This observation could be due to the continuous activation of CD4+ T cells where the cells are in a constant cyclic process of synthesis and shedding of CD40L after every 18 h. Hence, the observed trend at 72 h since 72 h is a multiple of 18 h.

The main criterion that is widely used to determine antigen-specificity and effector function of specific T cells is to identify the cytokine profile they produce in response to presented antigens. Studying autophagy appropriately in antigen-specific T cells (e.g., mycobacteria-specific CD4+T cells) would, thus require quantifying autophagy in the subset of cytokine-producing T cells after stimulation with antigen. Here we have demonstrated that autophagy could not be quantified in cytokine-specific CD4+ T cells using CytoID dye along with ICS. Our results show a complete loss of CytoID intensity after saponin permeabilization. As stated earlier, CytoID stains autophagosomes and autophagolysosome compartment, and autophagosome membranes have been suggested to arise from ER or Golgi (119), which are made-up of phospholipid biomembrane. Saponin which is the main constituent of permeabilization buffers are known to specifically interact with cholesterol in biomembranes, leading to selective removal of cholesterol from the phospholipid membranes while the membrane remains intact (120). Therefore, the action of saponin on cholesterol may have led to the leaking of the CytoID dye out of the autophagosomal or autophagolysosomal compartments, accounting for the loss of CytoID intensity. An attempted use of lower concentration of permeabilization buffer proved futile and thus showed similar result.

In order to study autophagy in antigen-specific CD4+T cells, which was not possible by combining CytoID dye and ICS, we have first attempted to indirectly correlate autophagy in activation marker expression cells to antigen-specific effector cytokines (IFN-γ, TNF-α and IL-2). T cells upregulate activation markers upon TCR stimulation (121) and TCR stimulation has been shown to induce autophagy and also lead to cytokine production in CD4+ T cells (22). Our data have shown that TCR stimulation of CD4+ T cells upregulated, as expected, activation markers CD40L, CD25 and CD69 expression. Autophagy analysis in these activation marker expressing cells suggested that they are the main cells which upregulate autophagy. This observation further confirmed that activation induces autophagy in CD4+ T cells. Basal level of autophagy observed in activation marker expressing cells at 24 h of stimulation could be due to the fact that autophagy upregulation in CD4+ T cells might purely be in response to energy need of the cell. Thus, at 24 h, CD4+ T cells might have had enough ATP stores to sustain for the cellular processes required during the

brief period (24 h) after TCR stimulation. Furthermore, T cell activation induces signaling through Akt/mTOR and mTOR activity is a known inhibitor of autophagy. Also, AMPK, a sensor of energy is known to respond to increasing AMP and calcium levels in cells. AMPK activates autophagy through the inhibition of mTOR and at the same time activating ULK1 signaling (37). Therefore, increasing levels of autophagy observed after 48 h may be due to increasing AMP and calcium levels after TCR stimulation, which might have triggered AMPK activation. Indeed, there is limited energy turnover in naive T cells. But upon stimulation, T cells need to generate enormous amounts of ATP for sustained growth and proliferation that follows and so, it is probable that activation of AMPK may allow T cells to switch on catabolic, ATP synthesis pathways (122).

While IFN-γ and IL-2 levels decreased at 48 h, autophagy still increased. As autophagy is needed for cytokine production, differentiation and proliferation (8, 19, 93), increased levels of autophagy suggest that maybe other cytokines, which were not characterized (e.g., IL-10) as well as the energy needed for proliferation and differentiation may be increasing. In sum, our results have shown that autophagy could indirectly be correlated to the level of effector cytokines (IFN-γ and IL-2) in activation marker CD25 expressing cells. This indirect correlation was finally confirmed by a novel method of analyzing autophagy in specific-cytokine (IFN-γ) producing cells using IFN-γ catch reagent. Analyzed results showed increased level of autophagy in CD25+IFN-γ+ cells compared to CD25+IFN-γ- cells. This suggest that more autophagy is induced in CD25+ activated T cells producing IFN-γ effector cytokine compared to CD25+ activated T cells that do not show IFN-γ cytokine production. IFN-γ synthesis could be an energy demanding cellular process, hence more autophagy was observed in IFN-γ producing CD4+CD25+ T cells.

Hypoxia has been shown to induce autophagy and this was mediated by HIF-1α (86). Our results have shown that hypoxia (2% O_2) alone does not induce autophagy in CD4+ T cells but rather upregulates TCR stimulation-induced autophagy. This effect may partly be the result of transient HIF-1α expression in CD4+ T cells under hypoxic condition, which could be upregulated or stabilized upon TCR stimulation. Indeed, it was demonstrated that HIF-1α protein synthesis is stabilized upon TCR stimulation and this effect may be enhanced under hypoxia (87). Therefore, we propose that in CD4+ T cells, TCR stimulation-induced autophagy is enhanced or upregulated by HIF-1α stabilization under hypoxia. This may partly be the result of increased synthesis of HIF-1α under hypoxia and its subsequent stabilization by TCR stimulation leading to autophagy

upregulation. This effect was corroborated by upregulated autophagy seen independent of IFN-γ production in CD4+CD25+T cells under hypoxia. Nonetheless, IFN-γ production partly influenced the level of autophagy seen under hypoxia and normoxia conditions. Furthermore, studies have shown that hypoxia enhances the secretion of CD4+ T cell effector cytokine IFN-γ (123). Our results have shown that IFN-γ and CD25 expression increased under hypoxic condition. This effect may partly be due to the stabilization of these lymphokine genes or proteins (IFN-γ and CD25) at the post-transcriptional or post-translational level (124), since the stabilization of CD25 and IFN-γ genes are known to enhance the expression of IFN-γ and CD25 (112, 113). The observation made under hypoxia is exciting even though only a single time point was analyzed. It would be interesting to follow-up on the effect hypoxia may have on activated CD4+ T cells over time, regarding IFN-γ, IL-2 and IL-10 production and the regulation of autophagy. In our experiment, hypoxia potently increased effector cytokine IFN-γ and autophagy levels. Therefore we would like to find out the role IL-10 induction might play on autophagy and IFN-γ secretion under hypoxia, since IL-10 is known to be induced in granuloma-associated infections and it inhibits autophagy (83, 89). Further, we do not really know how these CD4+ T cells would handle prolonged hypoxic stress, even though it was demonstrated that hypoxia induced autophagy in macrophage cell lines and mouse embryonic fibroblast enhances survival (86). Also, in peripheral T cells it was shown that HIF-1α, which is potently induced by TCR stimulation and enhanced by hypoxia, increases the survival of T cells through the HIF-1α-adrenomedullin signaling cascade (88). Not doubting these observations, however, one could speculate that the continuous high level of autophagy and effector cytokine (IFN-γ) production might lead to the exhaustion of these lymphocytes and subsequently to the demise of the cells. It has been demonstrated recently that excessive autophagy induced by a cell penetrating autophagy inducing peptide, Tat-Beclin 1, which is derived from the autophagy protein Beclin 1, induced autophagy dependent cell death (125). This type of cell death, known as autosis, has also been observed under pathophysiological conditions such as starvation.

With regards to studying autophagy regulation in mycobacteria-specific CD4+ T cells under hypoxia, our attempted expansion of mycobacteria-specific CD4+ T cells was successful. We observed the expression of effector Th1 cells cytokines IFN-γ, IL-2 and TNF-α, which are known to be produced in response to mycobacterial infection. These cytokines have been suggested to initiate the main events leading to Mtb control in immunocompetent individuals (73, 76, 126). Our results have shown high levels of IFN-γ production after 24 h of re-stimulation, which suggested

that expression of IFN-γ in CD4+ T may be relatively late compared to TNF-α and IL-2. The low expression of TNF-α and IL-2 suggested that they may be early produced cytokines. Indeed, it has been reported that TNF-α is the initial cytokine expressed in response to Mtb, followed by IFN-γ. In addition, expression of TNF-α was observed to peak at 8 h while IFN-γ was at 16 h (127). Also, IL-2 expression is transiently induced in activated T cells (114). We observed relatively more cytokines produced by CD4+ T cells expanded in the TexMACS medium, which is an optimized medium for T cell culture, than RPMI-complete media. This effect could be due to the fact that TexMACS media may have contained nutrient supplements which made CD4+T cells to thrive better during the expansion periods. However, more expansion experiments are needed to validate this observation. Using this expansion protocol we successfully expanded mycobacteria-specific CD4+ T cells from healthy donor to about 15 %, with successfully expanded mycobacteria-specific T cells showing Th1 cytokine profile. The mycobacteria-specific CD4+ T cell expansion protocol needs further optimization to reliably expand mycobacteria-specific CD4+ T cells from healthy donors. This is because, we were not able to detect mycobacteria-specific CD4+ T cells from all donors and we also encountered problems with generating reliable, good quality autologous MDMs required for re-stimulating the expanded CD4+ T cells. This would then allow for optimal successful expansion of primary mycobacteria-specific CD4+ T cells from healthy donors. The tools established in this study would then allow onward studies of autophagy and effector cytokine regulation in mycobacteria-specific CD4+ T cells under hypoxic conditions. Findings from these experiments might contribute to an improved understanding of the processes happening in the granulomas of TB patients.

6 Conclusion, recommendation and future perspectives

The hallmark of an immune response to Mtb is granuloma formation. The environment of the granuloma is hypoxic, which led to the suggestion that the relative hypoxia in the granuloma is a contributing factor to the latent infection phenotype and the associated relative resistance of Mtb to host effector mechanisms. Furthermore, autophagy has been suggested to play numerous roles in disease and development. Worthy of note is the involvement of autophagy in memory T cell formation and the regulation of cytokine production. Autophagy in general is a *de novo* intracellular protein and organelle degradation pathway in eukaryotic cells that has been suggested to be a stress sensor. There are currently no studies evaluating the impact hypoxia may play on autophagy in mycobacteria-specific CD4+ T cells as seen in the granuloma of TB patients. We now have novel tools available to directly study autophagy in different subsets of T cells. This tools would also allow us to study the regulation of autophagy, activation markers and effector cytokines in parallel.

In establishing this assay, most of the experiments were repeated twice. Therefore, we recommend a repetition of all these methods using biological and technical replicates in order to obtain statistical significant values. Expanded mycobacteria-specific CD4+ T cells were not fully optimized, since we encountered a lot of challenges trying to establish this assay. Therefore, we recommend that this assay should be fully optimized to allow for it use in studying autophagy under hypoxia. An aspect of the expansion protocol that needs to be fully optimized is the monocyte isolation step.

The tools developed in this study can be used to elucidate autophagy regulation in different subsets of mycobacteria-specific CD4+ T cells under hypoxic conditions, as seen in the granuloma of TB patients, when expansion protocol works efficiently. This assays can play valuable roles in elucidating the role *Salmonella typhi* granulomas may play in modulating CD4+ T cell responses. Also, this method can be used to assess the impact of atherosclerotic plaque and tumor microenvironment on the modulation of autophagy and effector cytokine in different subsets of antigen-specific T cells in atherosclerosis and cancer patients respectively. Furthermore, the assay

has the potential in helping us understand the impact of HIV and inflammasome activation on autophagy regulation in memory CD4+ T cells.

References

1. Jia, W., M.-X. He, I. X. McLeod, and Y.-W. He. 2013. Autophagy, a novel pathway to regulate calcium mobilization in T lymphocytes. *Front. Immunol.* 4: 179.

2. Puleston, D. J., and A. K. Simon. 2014. Autophagy in the immune system. *Immunology* 141: 1–8.

3. Valdor, R., and F. MacIan. 2012. Autophagy and the regulation of the immune response. *Pharmacol. Res.* 66: 475–483.

4. Schmid, D., and C. Münz. 2007. Innate and Adaptive Immunity through Autophagy. *Immunity* 27: 11–21.

5. Kaushik S. and Cuervo A.M. 2009. Chaperone-Mediated Autophagy. *Methods* 70: 1–17.

6. Cuervo, A. M., and E. Wong. 2014. Chaperone-mediated autophagy: roles in disease and aging. *Cell Res.* 24: 92–104.

7. Münz, C. 2009. Enhancing immunity through autophagy. *Annu. Rev. Immunol.* 27: 423–49.

8. Bronietzki, A. W., M. Schuster, and I. Schmitz. 2014. Autophagy in T-cell development, activation and differentiation. *Immunol. Cell Biol.* 1–10.

9. Tanida, I. 2011. Autophagosome formation and molecular mechanism of autophagy. *Antioxid. Redox Signal.* 14: 2201–14.

10. Xie, Y., R. Kang, X. Sun, M. Zhong, J. Huang, D. J. Klionsky, and D. Tang. 2014. Posttranslational modification of autophagy-related proteins in macroautophagy. *Autophagy* 37–41.

11. Kim, J., M. Kundu, B. Viollet, and K.-L. Guan. 2011. AMPK and mTOR regulate autophagy through direct phosphorylation of Ulk1. *Nat. Cell Biol.* 13: 132–141.

12. Kuballa, P., W. M. Nolte, A. B. Castoreno, and R. J. Xavier. 2012. Autophagy and the Immune System. *Annu. Rev. Immunol.* 30: 611–646.

13. Weidberg, H., E. Shvets, T. Shpilka, F. Shimron, V. Shinder, and Z. Elazar. 2010. LC3 and GATE-16/GABARAP subfamilies are both essential yet act differently in autophagosome biogenesis. *EMBO J.* 29: 1792–1802.

14. Wang, C.-W., and D. J. Klionsky. 2003. The Molecular Mechanism of Autophagy. *Mol. Med.* 9: 65–76.

15. Germain, R. N. 2002. T-cell development and the CD4-CD8 lineage decision. *Nat. Rev. Immunol.* 2: 309–322.

16. Godfrey, D. I., J. Kennedy, T. Suda, and a Zlotnik. 1993. A developmental pathway involving four phenotypically and functionally distinct subsets of CD3-CD4-CD8- triple-negative adult mouse thymocytes defined by CD44 and CD25 expression. *J. Immunol.* 150: 4244–4252.

17. Koch, U., and F. Radtke. 2011. Mechanisms of T Cell Development and Transformation. *Annu. Rev. Cell Dev. Biol.* 27: 539–562.

18. Klein, L., M. Hinterberger, G. Wirnsberger, and B. Kyewski. 2009. Antigen presentation in the thymus for positive selection and central tolerance induction. *Nat. Rev. Immunol.* 9: 833–844.

19. Pua, H. H., I. Dzhagalov, M. Chuck, N. Mizushima, and Y.-W. He. 2007. A critical role for the autophagy gene Atg5 in T cell survival and proliferation. *J. Exp. Med.* 204: 25–31.

20. Li, C., E. Capan, Y. Zhao, J. Zhao, D. Stolz, S. C. Watkins, S. Jin, and B. Lu. 2006. Autophagy Is Induced in CD4+ T Cells and Important for the Growth Factor-Withdrawal Cell Death. *J. Immunol.* 177: 5163–5168.

21. Gerland, L. M., L. Genestier, S. Peyrol, M. C. Michallet, S. Hayette, I. Urbanowicz, P. Ffrench, J. P. Magaud, and M. Ffrench. 2004. Autolysosomes accumulate during in vitro CD8+ T-lymphocyte aging and may participate in induced death sensitization of senescent cells. *Exp. Gerontol.* 39: 789–800.

22. Vanessa M. Hubbard, Rut Valdor, Bindi Patel, Rajat Singh, Ana Maria Cuervo, A., and F. Macian. 2009. Macroautophagy regulates energy metabolism during effector T cell activation. 27: 417–428.

23. McLeod, I. X., X. Zhou, Q.-J. Li, F. Wang, and Y.-W. He. 2011. The class III kinase Vps34 promotes T lymphocyte survival through regulating IL-7Rα surface expression. *J. Immunol.* 187: 5051–61.

24. Mattoo, H., M. Faulkner, U. Kandpal, R. Das, V. Lewis, A. George, S. Rath, J. M. Durdik, and V. Bal. 2009. Naive CD4 T cells from aged mice show enhanced death upon primary activation. *Int. Immunol.* 21: 1277–1289.

25. Copetti, T., C. Bertoli, E. Dalla, F. Demarchi, and C. Schneider. 2009. p65/RelA modulates BECN1 transcription and autophagy. *Mol. Cell. Biol.* 29: 2594–2608.

26. Jatin M. Vyas, A. G. V. der V. and H. L. P. 2012. The known unknowns of antigen processing and presentation. *Nat Rev Immunol* 29: 997–1003.

27. Crotzer, V. L., and J. S. Blum. 2010. Autophagy and adaptive immunity. *Immunology* 131: 9–17.

28. Schmid, D., M. Pypaert, and C. Münz. 2007. Antigen-Loading Compartments for Major Histocompatibility Complex Class II Molecules Continuously Receive Input from Autophagosomes. *Immunity* 26: 79–92.

29. Guermonprez, P., J. Valladeau, L. Zitvogel, C. Théry, and S. Amigorena. 2002. Antigen presentation and T cell stimulation by dendritic cells. *Annu. Rev. Immunol.* 20: 621–67.

30. English, L., M. Chemali, J. Duron, C. Rondeau, A. Laplante, D. Gingras, D. Alexander, D. Leib, C. Norbury, R. Lippé, and M. Desjardins. 2009. Autophagy enhances the presentation of endogenous viral antigens on MHC class I molecules during HSV-1 infection. *Nat. Immunol.* 10: 480–487.

31. Nimmerjahn, F., S. Milosevic, U. Behrends, E. M. Jaffee, D. M. Pardoll, G. W. Bornkamm, and J. Mautner. 2003. Major histocompatibility complex class II-restricted presentation of a cytosolic antigen by autophagy. *Eur. J. Immunol.* 33: 1250–1259.

32. Paludan, C., D. Schmid, M. Landthaler, M. Vockerodt, D. Kube, T. Tuschl, and C. Münz. 2005. Endogenous MHC class II processing of a viral nuclear antigen after autophagy. *Science* 307: 593–596.

33. Ní Cheallaigh, C., J. Keane, E. C. Lavelle, J. C. Hope, and J. Harris. 2011. Autophagy in the immune response to tuberculosis: clinical perspectives. *Clin. Exp. Immunol.* 164: 291–300.

34. Frauwirth, K. a., J. L. Riley, M. H. Harris, R. V. Parry, J. C. Rathmell, D. R. Plas, R. L. Elstrom, C. H. June, and C. B. Thompson. 2002. The CD28 signaling pathway regulates glucose metabolism. *Immunity* 16: 769–777.

35. Carr, E. L., A. Kelman, G. S. Wu, R. Gopaul, E. Senkevitch, A. Aghvanyan, A. M. Turay, and K. a Frauwirth. 2010. Glutamine uptake and metabolism are coordinately regulated by ERK/MAPK during T lymphocyte activation. *J. Immunol.* 185: 1037–1044.

36. Powell, J. D., C. G. Lerner, and R. H. Schwartz. 1999. Inhibition of cell cycle progression by rapamycin induces T cell clonal anergy even in the presence of costimulation. *J. Immunol.* 162: 2775–2784.

37. Tamás, P., S. a Hawley, R. G. Clarke, K. J. Mustard, K. Green, D. G. Hardie, and D. a Cantrell. 2006. Regulation of the energy sensor AMP-activated protein kinase by antigen receptor and Ca2+ in T lymphocytes. *J. Exp. Med.* 203: 1665–1670.

38. Kindt, T. J., R. A. Goldsby, and B. A. Osborne. 2007. *Kuby Immunology*,.

39. Fox, C. J., P. S. Hammerman, and C. B. Thompson. 2005. Fuel feeds function: energy metabolism and the T-cell response. *Nat. Rev. Immunol.* 5: 844–852.

40. Macián, F., F. García-Cózar, S. H. Im, H. F. Horton, M. C. Byrne, and A. Rao. 2002. Transcriptional mechanisms underlying lymphocyte tolerance. *Cell* 109: 719–731.

41. Macian, F. 2005. NFAT proteins: key regulators of T-cell development and function. *Nat. Rev. Immunol.* 5: 472–484.

42. Wang, D., R. Matsumoto, Y. You, T. Che, X.-Y. Lin, S. L. Gaffen, and X. Lin. 2004. CD3/CD28 costimulation-induced NF-kappaB activation is mediated by recruitment of protein kinase C-theta, Bcl10, and IkappaB kinase beta to the immunological synapse through CARMA1. *Mol. Cell. Biol.* 24: 164–171.

43. Smith-Garvin, J. E., G. a Koretzky, and M. S. Jordan. 2009. T cell activation. *Annu. Rev. Immunol.* 27: 591–619.

44. Padhan, K., and R. Varma. 2010. Immunological synapse: A multi-protein signalling cellular apparatus for controlling gene expression. *Immunology* 129: 322–328.

45. Lupino, E., C. Ramondetti, and M. Piccinini. 2012. IκB kinase β is required for activation of NF-κB and AP-1 in CD3/CD28-stimulated primary CD4(+) T cells. *J. Immunol.* 188: 2545–55.

46. Heissmeyer, V., and A. Rao. 2004. E3 ligases in T cell anergy--turning immune responses into tolerance. *Sci. STKE* 2004: pe29.

47. Taylor-Fishwick, D. A., and J. N. Siegel. 1995. Raf-1 provides a dominant but not exclusive signal for the induction of CD69 expression on T cells. *Eur. J. Immunol.* 25: 3215–3221.

48. Luckheeram, R. V., R. Zhou, A. D. Verma, and B. Xia. 2012. $CD4^{+}$T cells: differentiation and functions. *Clin. Dev. Immunol.* 2012: 925135.

49. Zhu, J., and W. E. Paul. 2008. CD4 T cells: fates, functions, and faults. *Blood* 112: 1557–69.

50. Crotty, S. 2011. Follicular helper CD4 T cells (TFH). *Annu. Rev. Immunol.* 29: 621–663.

51. Crotty, S. 2014. T Follicular Helper Cell Differentiation , Function , and Roles in Disease. *Immunity* 41: 529–542.

52. Gengenbacher, M., and S. H. E. Kaufmann. 2012. Mycobacterium tuberculosis: Success through dormancy. *FEMS Microbiol. Rev.* 36: 514–532.

53. Cooper, A. M. 2009. Cell-mediated immune responses in tuberculosis. *Annu. Rev. Immunol.* 27: 393–422.

54. Prezzemolo, T., G. Guggino, M. P. La Manna, D. Di Liberto, F. Dieli, and N. Caccamo. 2014. Functional Signatures of Human CD4 and CD8 T Cell Responses to Mycobacterium tuberculosis. *Front. Immunol.* 5: 180.

55. Bozzano, F., F. Marras, and A. De Maria. 2014. Immunology of tuberculosis. *Mediterr. J. Hematol. Infect. Dis.* 6: e2014027.

56. Who. 2014. Global tuberculosis report 2014 (WHO/HTM/TB/2014.08). .

57. Kleinnijenhuis, J., M. Oosting, L. a B. Joosten, M. G. Netea, and R. Van Crevel. 2011. Innate immune recognition of Mycobacterium tuberculosis. *Clin. Dev. Immunol.* 2011: 405310.

58. Hossain, M. M., and M.-N. Norazmi. 2013. Pattern recognition receptors and cytokines in Mycobacterium tuberculosis infection--the double-edged sword? *Biomed Res. Int.* 2013: 179174.

59. Ramakrishnan, L. 2012. Revisiting the role of the granuloma in tuberculosis. *Nat. Rev. Immunol.* 12: 352–366.

60. Elks, P. M., S. Brizee, M. van der Vaart, S. R. Walmsley, F. J. van Eeden, S. a. Renshaw, and A. H. Meijer. 2013. Hypoxia Inducible Factor Signaling Modulates Susceptibility to Mycobacterial Infection via a Nitric Oxide Dependent Mechanism. *PLoS Pathog.* 9: 1–16.

61. Clambey, E. T. 2014. Hypoxia and hypoxia-inducible factors as regulators of T cell development, differentiation, and function. 55: 58–70.

62. Aderem, a, and D. M. Underhill. 1999. Mechanisms of phagocytosis in macrophages. *Annu. Rev. Immunol.* 17: 593–623.

63. Rohde, K., R. M. Yates, G. E. Purdy, and D. G. Russell. 2007. Mycobacterium tuberculosis and the environment within the phagosome. *Immunol. Rev.* 219: 37–54.

64. Fang, F. C. 2004. Antimicrobial reactive oxygen and nitrogen species: concepts and controversies. *Nat. Rev. Microbiol.* 2: 820–832.

65. Van der Wel, N., D. Hava, D. Houben, D. Fluitsma, M. van Zon, J. Pierson, M. Brenner, and P. J. Peters. 2007. M. tuberculosis and M. leprae translocate from the phagolysosome to the cytosol in myeloid cells. *Cell* 129: 1287–98.

66. Songane, M., J. Kleinnijenhuis, M. G. Netea, and R. van Crevel. 2012. The role of autophagy in host defence against Mycobacterium tuberculosis infection. *Tuberculosis (Edinb).* 92: 388–96.

67. Petruccioli, E., A. Romagnoli, M. Corazzari, E. M. Coccia, O. Butera, G. Delogu, M. Piacentini, E. Girardi, G. M. Fimia, and D. Goletti. 2012. Specific T cells restore the autophagic flux inhibited by Mycobacterium tuberculosis in human primary macrophages. *J. Infect. Dis.* 205: 1425–35.

68. Lanzavecchia, a, and F. Sallusto. 2000. Dynamics of T lymphocyte responses: intermediates, effectors, and memory cells. *Science* 290: 92–97.

69. Sallusto, F., J. Geginat, and A. Lanzavecchia. 2004. Central memory and effector memory T cell subsets: function, generation, and maintenance. *Annu. Rev. Immunol.* 22: 745–763.

70. Wolf, A. J., L. Desvignes, B. Linas, N. Banaiee, T. Tamura, K. Takatsu, and J. D. Ernst. 2008. Initiation of the adaptive immune response to Mycobacterium tuberculosis depends on antigen production in the local lymph node, not the lungs. *J. Exp. Med.* 205: 105–115.

71. Gupta, A., A. Kaul, A. G. Tsolaki, U. Kishore, and S. Bhakta. 2012. Mycobacterium tuberculosis: immune evasion, latency and reactivation. *Immunobiology* 217: 363–74.

72. Roberts, L. L., and C. M. Robinson. 2014. Mycobacterium tuberculosis infection of human dendritic cells decreases integrin expression, adhesion and migration to chemokines. *Immunology* 141: 39–51.

73. Green, A. M., R. Difazio, and J. L. Flynn. 2013. IFN-γ from CD4 T cells is essential for host survival and enhances CD8 T cell function during Mycobacterium tuberculosis infection. *J. Immunol.* 190: 270–7.

74. Geldmacher, C., N. Ngwenyama, A. Schuetz, C. Petrovas, K. Reither, E. J. Heeregrave, J. P. Casazza, D. R. Ambrozak, M. Louder, W. Ampofo, G. Pollakis, B. Hill, E. Sanga, E. Saathoff, L. Maboko, M. Roederer, W. a Paxton, M. Hoelscher, and R. a Koup. 2010. Preferential infection and depletion of Mycobacterium tuberculosis-specific CD4 T cells after HIV-1 infection. *J. Exp. Med.* 207: 2869–2881.

75. Haug, M., J. a. Awuh, M. Steigedal, J. Frengen Kojen, A. Marstad, I. S. Nordrum, Ø. Halaas, and T. H. Flo. 2013. Dynamics of immune effector mechanisms during infection with mycobacterium avium in C57BL/6 mice. *Immunology* 140: 232–243.

76. Dorhoi, A., and S. H. E. Kaufmann. 2014. Tumor necrosis factor alpha in mycobacterial infection. *Semin. Immunol.* 26: 203–9.

77. Matucci, A., E. Maggi, and A. Vultaggio. 2014. Cellular and humoral immune responses during tuberculosis infection: useful knowledge in the era of biological agents. *J. Rheumatol. Suppl.* 91: 17–23.

78. Casanova, J.-L., and L. Abel. 2002. Genetic dissection of immunity to mycobacteria: the human model. *Annu. Rev. Immunol.* 20: 581–620.

79. Flynn, J. L. 1993. An essential role for interferon gamma in resistance to Mycobacterium tuberculosis infection. *J. Exp. Med.* 178: 2249–2254.

80. Scanga, C., and V. Mohan. 2001. The inducible nitric oxide synthase locus confers protection against aerogenic challenge of both clinical and laboratory strains of Mycobacterium tuberculosis in mice. *Infect. Immun.* 69: 7711–7717.

81. Saliu, O. Y., C. Sofer, D. S. Stein, S. K. Schwander, and R. S. Wallis. 2006. Tumor-necrosis-factor blockers: differential effects on mycobacterial immunity. *J. Infect. Dis.* 194: 486–492.

82. Lünemann, J. D., and C. Münz. 2009. Autophagy in CD4+ T-cell immunity and tolerance. *Cell Death Differ.* 16: 79–86.

83. Harris, J., S. a. De Haro, S. S. Master, J. Keane, E. a. Roberts, M. Delgado, and V. Deretic. 2007. T Helper 2 Cytokines Inhibit Autophagic Control of Intracellular Mycobacterium tuberculosis. *Immunity* 27: 505–517.

84. Gutierrez, M., S. Master, and S. Singh. 2004. Autophagy Is a Defense Mechanism Inhibiting BCG and Mycobacterium tuberculosis Survival in Infected Macrophages. *Cell* 119: 753–766.

85. Via, L. E., P. L. Lin, S. M. Ray, J. Carrillo, S. S. Allen, Y. E. Seok, K. Taylor, E. Klein, U. Manjunatha, J. Gonzales, G. L. Eun, K. P. Seung, J. a. Raleigh, N. C. Sang, D. N. McMurray, J. L. Flynn, and C. E. Barry. 2008. Tuberculous granulomas are hypoxic in guinea pigs, rabbits, and nonhuman primates. *Infect. Immun.* 76: 2333–2340.

86. Bellot, G., R. Garcia-Medina, P. Gounon, J. Chiche, D. Roux, J. Pouysségur, and N. M. Mazure. 2009. Hypoxia-induced autophagy is mediated through hypoxia-inducible factor induction of BNIP3 and BNIP3L via their BH3 domains. *Mol. Cell. Biol.* 29: 2570–2581.

87. Nakamura, H., Y. Makino, K. Okamoto, L. Poellinger, K. Ohnuma, C. Morimoto, and H. Tanaka. 2005. TCR Engagement Increases Hypoxia-Inducible Factor-1 Protein Synthesis via Rapamycin-Sensitive Pathway under Hypoxic Conditions in Human Peripheral T Cells. *J. Immunol.* 174: 7592–7599.

88. Makino, Y., H. Nakamura, E. Ikeda, K. Ohnuma, K. Yamauchi, Y. Yabe, L. Poellinger, Y. Okada, C. Morimoto, and H. Tanaka. 2003. Hypoxia-inducible factor regulates survival of antigen receptor-driven T cells. *J. Immunol.* 171: 6534–6540.

89. Singh, a. K., and N. R. Thirumalapura. 2014. Early Induction of Interleukin-10 Limits Antigen-Specific CD4+ T Cell Expansion, Function, and Secondary Recall Responses during Persistent Phagosomal Infection. *Infect. Immun.* 82: 4092–4103.

90. Gazzinelli, R. T., M. Wysocka, S. Hieny, T. Scharton-Kersten, A. Cheever, R. Kühn, W. Müller, G. Trinchieri, and A. Sher. 1996. In the absence of endogenous IL-10, mice acutely infected with Toxoplasma gondii succumb to a lethal immune response dependent on CD4+ T cells and accompanied by overproduction of IL-12, IFN-gamma and TNF-alpha. *J. Immunol.* 157: 798–805.

91. O'Garra, A., and P. Vieira. 2007. T(H)1 cells control themselves by producing interleukin-10. *Nat. Rev. Immunol.* 7: 425–428.

92. Park, H. J., S. J. Lee, S. H. Kim, J. Han, J. Bae, S. J. Kim, C. G. Park, and T. Chun. 2011. IL-10 inhibits the starvation induced autophagy in macrophages via class I phosphatidylinositol 3-kinase (PI3K) pathway. *Mol. Immunol.* 48: 720–727.

93. Xu, X., K. Araki, S. Li, J.-H. Han, L. Ye, W. G. Tan, B. T. Konieczny, M. W. Bruinsma, J. Martinez, E. L. Pearce, D. R. Green, D. P. Jones, H. W. Virgin, and R. Ahmed. 2014. Autophagy is essential for effector CD8+ T cell survival and memory formation. *Nat. Immunol.* 15: 1–12.

94. Bennett, S., and S. N. Breit. 1994. Variables in the isolation and culture of human monocytes that are of particular relevance to studies of HIV. *J. Leukoc. Biol.* 56: 236–240.

95. Jørgensen, K., M. Skrede, V. Cruciani, S. O. Mikalsen, A. Slipicevic, and V. A. Flørenes. 2005. Phorbol ester phorbol-12-myristate-13-acetate promotes anchorage- independent growth and survival of melanomas through MEK-independent activation of ERK1/2. *Biochem. Biophys. Res. Commun.* 329: 266–274.

96. Chatila, T., L. Silverman, R. Miller, and R. Geha. 1989. Mechanisms of T cell activation by the calcium ionophore ionomycin. *J. Immunol.* 143: 1283–1289.

97. Raveche, E. 2010. Introduction to Flow Cytometry. 3–21.

98. Brown, M., and C. Wittwer. 2000. Flow cytometry: Principles and clinical applications in hematology. *Clin. Chem.* 46: 1221–1229.

99. Ormerod, M. G. 2000. *Flow Cytometry: A Practical Approach*, 3rd ed. Oxford Univ Press.

100. Sharrow, S. O. 2002. Overview of flow cytometry. *Curr. Protoc. Immunol.* Chapter 5: Unit 5.1.

101. Maecker, H. T., and J. Trotter. 2006. Flow cytometry controls, instrument setup, and the determination of positivity. *Cytometry. A* 69: 1037–42.

102. Howat, W. J., and B. a Wilson. 2014. Tissue fixation and the effect of molecular fixatives on downstream staining procedures. *Methods* 70: 12–19.

103. Mahmood, T., and P. C. Yang. 2012. Western blot: Technique, theory, and trouble shooting. *N. Am. J. Med. Sci.* 4: 429–434.

104. Demishtein, A., Z. Porat, Z. Elazar, and E. Shvets. 2015. Applications of flow cytometry for measurement of autophagy. *Methods* .

105. Barth, S., D. Glick, and K. F. Macleod. 2010. Autophagy: Assays and artifacts. *J. Pathol.* 221: 117–124.

106. Sakaki, K., and R. J. Kaufman. 2008. Regulation of ER stress-induced macroautophagy by protein kinase C. *Autophagy* 4: 841–843.

107. Hammond, A. S., S. J. McConkey, P. C. Hill, S. Crozier, M. R. Klein, R. a Adegbola, S. Rowland-Jones, R. H. Brookes, H. Whittle, and A. Jaye. 2008. Mycobacterial T cell responses in HIV-infected patients with advanced immunosuppression. *J. Infect. Dis.* 197: 295–299.

108. Silva Miranda, M., A. Breiman, S. Allain, F. Deknuydt, and F. Altare. 2012. The tuberculous granuloma: an unsuccessful host defence mechanism providing a safety shelter for the bacteria? *Clin. Dev. Immunol.* 2012: 139127.

109. Feng, Y., D. He, Z. Yao, and D. J. Klionsky. 2014. The machinery of macroautophagy. *Cell Res.* 24: 24–41.

110. Daoussis, D., A. P. Andonopoulos, and S. C. Liossis. 2004. Targeting CD40L : a Promising Therapeutic Approach. *Society* 11: 635–641.

111. Ortiz, A. M., R. Garcia-Vicuna, D. Sancho, A. Laffon, F. Sanchez-Madrid, and I. Gonzalez-Alvaro. 2000. Cyclosporin A inhibits CD69 expression induced on synovial fluid and peripheral blood lymphocytes by interleukin 15. *J. Rheumatol.* 27: 2329–2338.

112. Bryan, R. G., Y. Li, J. H. Lai, M. Van, N. R. Rice, R. R. Rich, and T. H. Tan. 1994. Effect of CD28 signal transduction on c-Rel in human peripheral blood T cells. *Mol. Cell. Biol.* 14: 7933–7942.

113. Fraser, J. D., and a Weiss. 1992. Regulation of T-cell lymphokine gene transcription by the accessory molecule CD28. *Mol. Cell. Biol.* 12: 4357–4363.

114. Fujimura, K., A. Oyamada, Y. Iwamoto, Y. Yoshikai, and H. Yamada. 2013. CD4 T cell-intrinsic IL-2 signaling differentially affects Th1 and Th17 development. *J. Leukoc. Biol.* 94: 271–9.

115. Cantrell, D. a, M. K. Collins, and M. J. Crumpton. 1988. Autocrine regulation of T-lymphocyte proliferation: differential induction of IL-2 and IL-2 receptor. *Immunology* 65: 343–349.

116. Cerdan, C., Y. Martin, M. Curcou, C. Mawas, and F. Birg. 1995. Costimulation Up-Regulates Long-Term. *Immunology* .

117. Rubinsztein, D. C., A. M. Cuervo, B. Ravikumar, S. Sarkar, V. Korolchuk, S. Kaushik, and D. J. Klionsky. 2009. In search of an "autophagomometer." *Autophagy* 5: 585–589.

118. Butler, D. 2008. How to interpret LC3 immunoblotting. *Autophagy* 37–41.

119. Tooze, S. a, and T. Yoshimori. 2010. The origin of the autophagosomal membrane. *Nat. Cell Biol.* 12: 831–835.

120. Jacob, M. C., M. Favre, and J. C. Bensa. 1991. Membrane cell permeabilization with saponin and multiparametric analysis by flow cytometry. *Cytometry* 12: 550–558.

121. Caruso, a., S. Licenziati, M. Corulli, a. D. Canaris, M. a. De Francesco, S. Fiorentini, L. Peroni, F. Fallacara, F. Dima, a. Balsari, and a. Turano. 1997. Flow cytometric analysis of

activation markers on stimulated T cells and their correlation with cell proliferation. *Cytometry* 27: 71–76.

122. Towler, M. C., and D. G. Hardie. 2007. AMP-activated protein kinase in metabolic control and insulin signaling. *Circ. Res.* 100: 328–341.

123. Roman, J., T. Rangasamy, J. Guo, S. Sugunan, N. Meednu, G. Packirisamy, L. a. Shimoda, A. Golding, G. Semenza, and S. N. Georas. 2010. T-cell activation under hypoxic conditions enhances IFN-γ secretion. *Am. J. Respir. Cell Mol. Biol.* 42: 123–128.

124. Young, H. A., and J. H. Bream. 2007. IFN-gamma: recent advances in understanding regulation of expression, biological functions, and clinical applications. *Curr. Top. Microbiol. Immunol.* 316: 97–117.

125. Liu, Y., S. Shoji-Kawata, R. M. Sumpter, Y. Wei, V. Ginet, L. Zhang, B. Posner, K. a Tran, D. R. Green, R. J. Xavier, S. Y. Shaw, P. G. H. Clarke, J. Puyal, and B. Levine. 2013. Autosis is a Na+,K+-ATPase-regulated form of cell death triggered by autophagy-inducing peptides, starvation, and hypoxia-ischemia. *Proc. Natl. Acad. Sci. U. S. A.* 110: 20364–71.

126. Scanga, C. a, V. P. Mohan, K. Yu, H. Joseph, K. Tanaka, J. Chan, and J. L. Flynn. 2000. Depletion of CD4(+) T cells causes reactivation of murine persistent tuberculosis despite continued expression of interferon gamma and nitric oxide synthase 2. *J. Exp. Med.* 192: 347–358.

127. Antas, P. R. Z., J. S. Sales, K. C. Pereira, E. B. Oliveira, K. S. Cunha, E. N. Sarno, and E. P. Sampaio. 2004. Patterns of intracellular cytokines in CD4 and CD8 T cells from patients with mycobacterial infections. *Braz. J. Med. Biol. Res.* 37: 1119–29.

Web references

Spectral overlap between fluorescein isothiocyanate (FITC) and phycoerythrin (PE) fluorochromes after excitation. Retrieved from AppliedCytometry

Lymphoprep desity gradient isolation protocol information. Retrieved from Axis-shield density gradient media leaflet

Miltenyi human CD4+ isolation kit data sheet. Retrieved from (Miltenyi human CD4+ isolation kit data sheet

CytoID Autophagy detection kit. Retrieved from CytoID autophagy detection kit product manual

IFN-γ Secretion Assay-Cell Enrichment kit. Retrieved from IFN Secretion assay-cell Enrichment and Detection kit data sheet

Appendices

Appendix I: MACS columns needed for the number of starting cells

MACS Columns and MACS Separators: Choose the appropriate MACS Separator and MACS Columns according to the number of labeled cells and to the number of total cells.

Column	Max. number of labeled cells	Max. number of total cells	Separator
LS	10^8	2×10^9	MidiMACS, QuadroMACS, VarioMACS, SuperMACS II
XS	10^9	2×10^{10}	SuperMACS II
autoMACS	2×10^8	4×10^9	autoMACS Pro, autoMACS

▲ **Note:** Column adapters are required to insert certain columns into the VarioMACS™ or SuperMACS™ II Separators. For details refer to the respective MACS Separator data sheet.

Appendix II: Buffers and solutions used in immunoblotting

Buffer	Stock solution	Volume
Lysis buffer 2X Storage: - 20 °C Diluted 1:1 with freshly prepared benzonase and proteinase inhibitor cocktail	 Glycerol 87% NaF 0.5M Tris/HCL pH 8.0, 1 M EDTA pH 8.0, 0.2M EGTA 0.2M NaCl 5M Triton X-100 10% Na_3VO_4 0.2M Sodium Deoxychelat 10% MiliQ water	Total volume: 100 ml 23 ml 20 ml 10 ml 1 ml 1 ml 15.4 ml 20 ml 1 ml 10 ml 10 ml Up to 100 ml
Benzonase and proteinase inhibitor cocktail	 Benzonase 0.25 U/ml Proteinase inhibitor cocktail MiliQ water	Total volume: 5 ml 1.3 µl 1 tablet 5 ml
Tris buffered saline with Tween	 Tris (pH 7.5) 1M Tween-20 NaCl 5M Deionised water	Total volume: 1000ml 9.9 ml 1 ml 19.8 ml Up to 1000 ml

Appendix III: Purity of isolated CD4+ Tcell

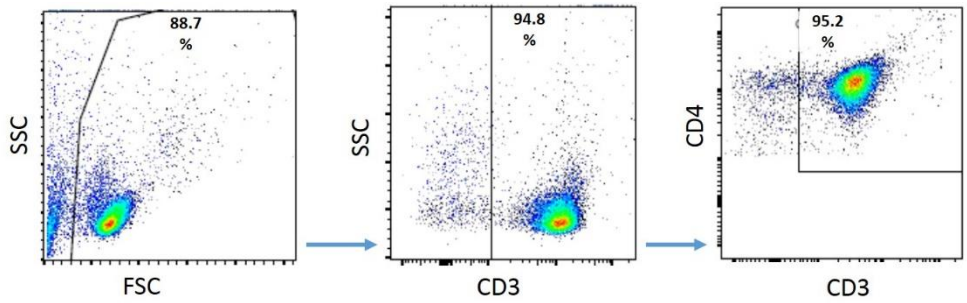

The gate defined is representative of how purity was assessed in all isolated CD4+ Tcells used in this project. FSC and SSC gates were defined on the lymphocyte population followed by CD3+ gating and then CD4+CD3+ gate.

Appendix IV: Effect of different fixation and permeabilization buffer on activated CD4+ Tcells.

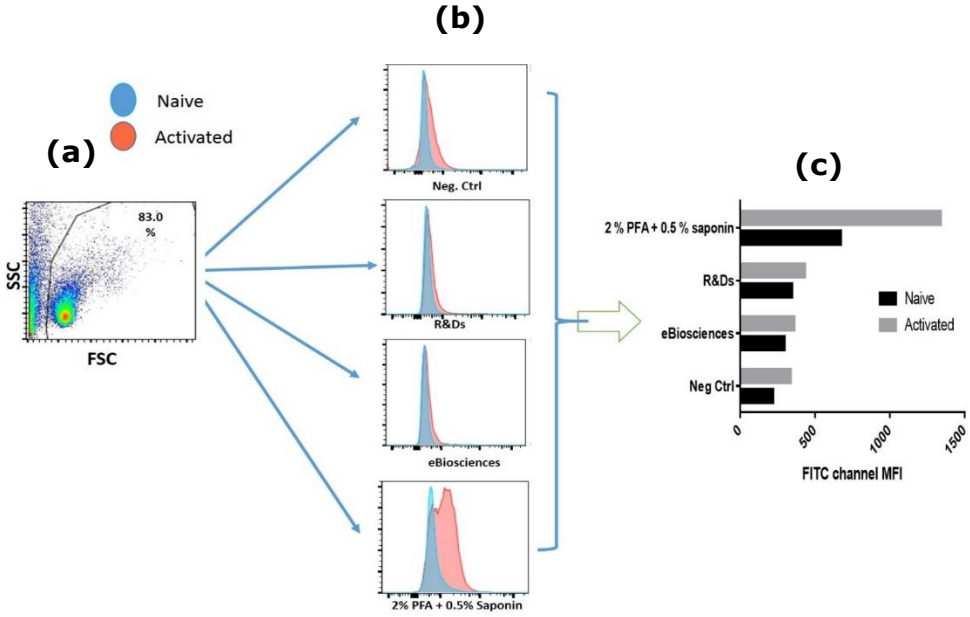

Effects of different fixation/permeabilization buffers in CytoID (FITC) channel. (a) Represents the forward and side scatter plot, (b) is the overlay histogram for unstimulated (blue) and activated (red) cells treated with the various fixation/permeabilization buffers and (c) is the quantified MFI in FITC channel. Cells were treated with the various fixation/permeabilization buffer after 48 h of

activation. Neg. Ctrl is representative of cells with no fixation/permeabilization buffer treatment. R&Ds and eBiosciences represents fixation/permeabilzation buffers from these manufactures.

Appendix V: Assessing the effect of protein transport inhibitor (PTI) cocktail on autophagy induction after 5 h of culturing with stimulated CD4+ Tcells

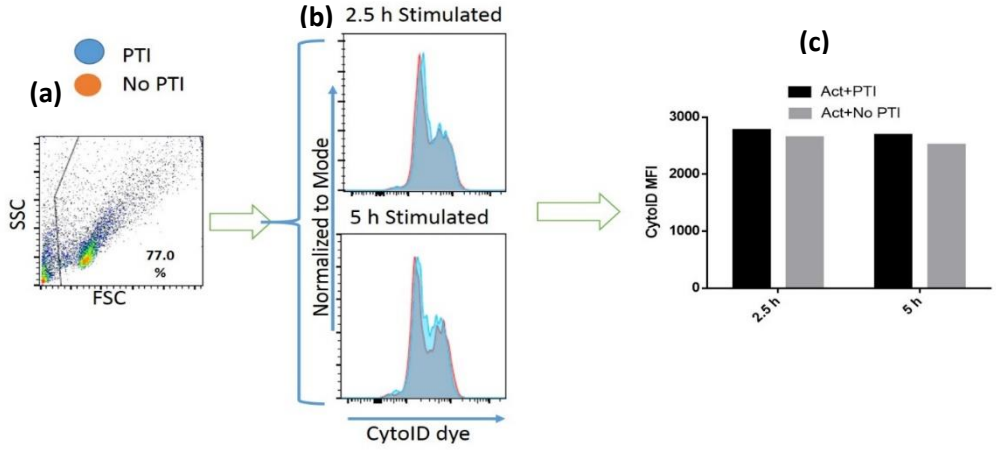

There seems to be no effect on autophagy after 5 h of CD4+ Tcell treatment with PTI. (a) Lymphocyte gate (b) overlay of histogram plots for various time point treatment. (c) CytoID MFI for the various time point. Cells were treated with PTI after 48 h of stimulation.

Appendix VI: CytoID histogram overlay for CD25+CD69-, CD25+CD69+, CD25-CD69+ and CD25-CD69- cells after 48 h stimulation with plate bound aCD3/28